



ChemComm

**Beyond Darunavir: Recent Development of Next Generation
HIV-1 Protease Inhibitors to Combat Drug Resistance**

Journal:	<i>ChemComm</i>
Manuscript ID	CC-FEA-08-2022-004541.R1
Article Type:	Feature Article

SCHOLARONE™
Manuscripts

ARTICLE

Beyond Darunavir: Recent Development of Next Generation HIV-1 Protease Inhibitors to Combat Drug Resistance

Arun K. Ghosh,^{*a} Irene T. Weber^b and Hiroaki Mitsuya^{c,d,e}

Received 00th January 20xx,
Accepted 00th January 20xx

DOI: 10.1039/x0xx00000x

We report our recent development of a conceptually new generation of exceptionally potent non-peptidic HIV-1 protease inhibitors that displayed excellent pharmacological and drug-resistance profiles. Our X-ray structural studies of darunavir and other designed inhibitors from our laboratories led us to create a variety of inhibitors incorporating fused ring polycyclic ethers and aromatic heterocycles to promote hydrogen bonding interactions with the backbone atoms of HIV-1 protease as well as van der Waals interactions with residues in the S2 and S2' subsites. We have also incorporated specific functionalities to enhance van der Waals interactions in the S1 and S1' subsites. The combined effects of these structural templates are critical to the inhibitors' exceptional potency and drug-like properties. We highlight here our molecular design strategies to promote backbone hydrogen bonding interactions to combat drug-resistance and specific design of polycyclic ether templates to mimic peptide-like bonds in the HIV-1 protease active site. Our medicinal chemistry and drug development efforts led to the development of new generation inhibitors significantly improved over darunavir and displaying unprecedented antiviral activity against multidrug-resistant HIV-1 variants.

Introduction

The treatment of Acquired Immunodeficiency Syndrome (AIDS) continues to be a major challenge in medicine.^{1,2} According to the UNAIDS/WHO's 2021 report on HIV/AIDS, an estimated 38.4 million people globally are currently living with HIV-1 infection and an estimated 40.1 million people have died from AIDS-related illness since the start of the epidemic.^{3,4} The advent of highly active antiretroviral therapy (ART) in the mid-1990s, marked the beginning of a new era of treatment for patients with HIV-1 infection and AIDS.^{5,6} The ART treatment regimen is a combination therapy with HIV-1 protease inhibitor (PI) and reverse transcriptase inhibitor drugs.^{7,8} ART has significantly reduced morbidity and mortality associated with HIV-1 infection and AIDS. It has also improved the quality of life of patients who have access to these therapies. The use of ART dramatically transformed HIV/AIDS from a fatal disease to a manageable chronic disorder.^{9,10}

Despite the major clinical benefits of ART, initial protease inhibitor-based drugs possessed many detriments including peptide-like features, drug-related side-effects, and poor ADME properties.^{11,12} The rapid emergence of drug resistance often

quickly renders a selected treatment ineffective within a short period of time. Furthermore, HIV-associated neurocognitive disorder (HAND) is affecting nearly fifty percent of the current HIV-positive population.¹³ These problems seriously complicate the long-term management of HIV-1 infection and prevention of AIDS-related deaths.^{14,15} Over the years, our laboratories have focused on the design of a conceptually new generation of nonpeptide HIV-1 protease inhibitors that would maintain potent antiviral activity against multidrug-resistant HIV-1 variants and show improved pharmacological properties over existing PI-drugs.^{16,17} Our research efforts led to the design and discovery of a range of highly potent HIV-1 protease inhibitors that incorporated novel ligands and templates by drawing inspiration from natural products.^{18,19} One of these protease inhibitors is darunavir (DRV, **1**, Figure 1) which displayed drug-like properties and maintained potent antiviral activity against a wide range of highly multidrug-resistant HIV-1 variants.²⁰⁻²² Darunavir received FDA approval in 2006 for the treatment of patients harboring highly drug-resistant viruses.^{23,24} Subsequently, it received approval as a first-line therapy for treatment of all HIV/AIDS patients including pediatrics in the current US Department of Health and Human Service (DHHS) guidelines.^{25,26}

One of the intriguing features of darunavir is the presence of a stereochemically defined and conformationally constrained bicyclic *bis*-tetrahydrofuran (*bis*-THF) heterocycle.^{27,28} The X-ray structure of DRV-bound HIV-1 protease revealed that both oxygens of the *bis*-THF form very strong hydrogen bonds with the Asp29 and Asp30 backbone amide NHs at the S2 subsite of HIV-1 protease.^{29,30} The bicyclic ring system of the *bis*-THF ligand forms van der Waals interactions with residues in the S2 subsite.^{18,31,32} The P2' ligand, 4-amino sulfonamide was also

^a Prof. Dr. A. K. Ghosh, Department of Chemistry and Department of Medicinal Chemistry, Purdue University, West Lafayette, IN 47907, E-mail: akghosh@purdue.edu

^b Prof. Dr. I. T. Weber, Departments of Biology and Chemistry, Molecular Basis of Disease, Georgia State University, Atlanta, GA 30303

^c Dr. H. Mitsuya, Departments of Hematology and Infectious Diseases, Kumamoto University School of Medicine, Kumamoto 860-8556, Japan

^d Dr. H. Mitsuya, Experimental Retrovirology Section, HIV and AIDS Malignancy Branch, National Cancer Institute, Bethesda, MD 20892

^e Dr. H. Mitsuya, Center for Clinical Sciences, National Center for Global Health and Medicine, Shinjuku, Tokyo 162-8655, Japan

specifically chosen to promote hydrogen bonding interactions with the backbone atoms at the S2' subsite.^{18,29} The overall structural features of darunavir, its molecular interactions with HIV-1 protease particularly its network of hydrogen bonding interactions with backbone atoms, and its ability to maintain robust antiviral activity with multidrug-resistant HIV-1 variants further stimulated our molecular design of novel scaffolds and templates for further improving inhibitor properties. Herein, we provide highlights of our recent design of new generation HIV-1 protease inhibitors that incorporated unprecedented 6-5-5 ring-fused tetrahydropyrano-furan derivatives as the P2 ligand in combination with alkylaminobenzoxazole and thiazole derivatives as the P2'-ligand. These inhibitors are specifically designed to maximize interactions including van der Waals interactions and hydrogen bonding interactions with the HIV-1 protease backbone atoms to combat drug resistance.

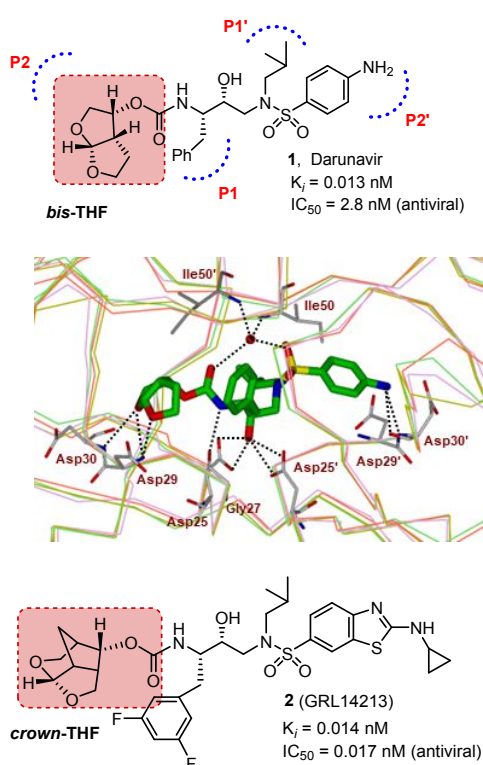


Figure 1. Structure and activity of inhibitors 1 and 2 (PDB: 21EN).

Promoting Backbone Hydrogen Bonding Interactions: Molecular Design Strategy to Combat Drug-Resistance

The underlying principle for our structure-based design of inhibitors to combat drug resistance involves maximizing an inhibitor's active site interactions, particularly with backbone atoms from the S2 to S2' subsites.^{29,33,34} We have critically analyzed and compared various mutant HIV-1 protease X-ray structures with wild-type HIV-1 protease and observed that the active site backbone conformation of these mutant proteases is only distorted minimally compared to wild-type HIV-1

protease.^{35,36} It is likely that the protease enzyme cannot significantly alter its active site backbone conformation without compromising its catalytic fitness and efficiency required for viral replication. Therefore, our "backbone binding" inhibitor design strategy to combat drug-resistance has evolved to maximize interactions including van der Waals interactions and hydrogen-bonding interactions with the active site of HIV-1 protease.^{29,34} In principle, such an inhibitor would likely maintain these key interactions including hydrogen-bonds with the backbone atoms of protease mutants. As a consequence, the development of drug-resistant HIV-1 variants would be reduced as altering backbone conformation would lead to impaired proteolysis of the natural polyprotein substrates. Our simplified view is to design an inhibitor like a 'molecular crab' that would tightly grip the protein backbone and hold on to the enzyme active site.³⁴ HIV-1 protease is an aspartic acid protease. The active form of HIV-1 protease is a homodimer containing two catalytic aspartic acid residues in the active site. Our model for inhibitor design to combat drug resistance is shown in Figure 2.³³ An inhibitor would have a functional group that would mimic the transition-state of the scissile bond cleavage. Among many known transition-state mimetics, we selected (*R*)-hydroxyethylamine sulfonamide dipeptide isostere with a hydroxyl group with (*R*)-configuration to bind the catalytic aspartates.^{28,37} The P1 and P1' ligands would fill in the hydrophobic S1 and S2 subsites and P2 and P2' ligands would interact with the S2 and S2' subsites through robust hydrogen bonding interactions with the backbone atoms as well as van der Waals interactions with the residues.



Figure 2. Design models for PIs to combat drug resistance. Promote robust hydrogen bonds through the P2- and P2'-ligands in both the S2 and S2'-subsites. The hydroxyl group to bind to catalytic aspartates mimicking transition-state, and the P1 and P1'-ligands to fill in the S1 and S1'-subsites.

Using our "backbone binding" design strategy, we have recently created a range of exceptionally potent HIV-1 protease inhibitors that incorporated polycyclic ethers as P2 ligands and heterocyclic sulfonamide derivatives as the P2' ligands. These compounds have shown exceptional antiviral activity against a range of highly multidrug-resistant HIV-1 variants. Through X-ray structural studies and analysis of antiviral activity, we can corroborate our backbone binding molecular design strategy as a powerful design concept to combat drug resistance.^{19,29,34}

Cyclic Ether Templates from Natural products: Inhibitor Design Strategies to Mimic peptide bonds.

Historically, natural products have been important sources for structurally diverse bioactive molecules enabling discovery and development of new drugs.^{38,39} Fine-tuning and optimization over millions of years of evolution, organisms have biosynthesized a variety of structurally intriguing molecules and molecular templates, specifically custom-made to interact and maintain their activity in biological microenvironments.⁴⁰ We became motivated to harness some of nature's molecular templates in our design of new nonpeptide inhibitors, considering the evolutionary fitness and stability of these functionalities. We are particularly intrigued by the cyclic ether and cyclic acetal structural features of numerous bioactive natural products.^{16,17} As shown in Figure 3, ginkgolides (**3**), isolated from predinosaur era tree, *Ginkgo biloba* are used as dietary supplements for human health.⁴¹ Laulimalide (**4**), isolated from marine sponge, exhibits potent anticancer activity.^{42,43} Azadirachtin (**5**), isolated from *Azadirachta indica*, has shown broad-spectrum insecticide properties.⁴⁴ Platensimycin, isolated from *Streptomyces platensis* is a potent broad-spectrum antibiotic.^{45,46} Eribulin mesylate (**7**, Halven®), is a semi-synthetic derivative of halichondrin B and is used as an approved anticancer drug.⁴⁷ As can be seen, these bioactive natural products possess an abundant amount of cyclic ether structural features.

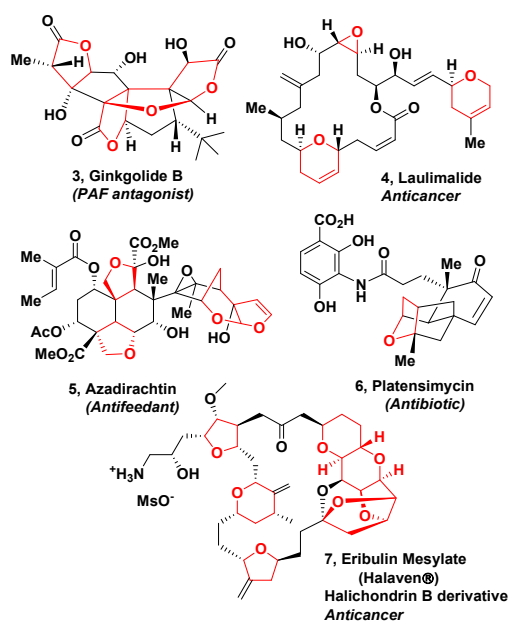


Figure 3. Structure of ginkgolide (**3**), laulimalide (**4**), azadirachtin (**5**), platensimycin (**6**), and Erlbulin (**7**) natural products

The cyclic ether functionalities in these molecules are critically important for their biological activity. Presumably, the cyclic ether oxygen is positioned to make up to two hydrogen bonding interactions with target peptide or protein residues in the drug binding site. The side chain substituents around the cyclic ether functionality are likely mimicking the side chains of

peptides and proteins. Numerous X-ray structural studies of cyclic ether-derived natural products with target enzymes or receptors revealed that these structural features not only provide overall shape and geometry of the molecules, they also serve as important pharmacophores and make critical interactions with their respective biological target proteins.^{48,49} An X-ray crystal structure (PDB code: 404H) of laulimalide (**4**) and β -tubulin, with its target protein show these critical interactions.⁵⁰ As shown in Figure 4, the tetrahydropyran ring oxygen in the macrocycle forms a strong hydrogen bond with the side chain of Asn339.

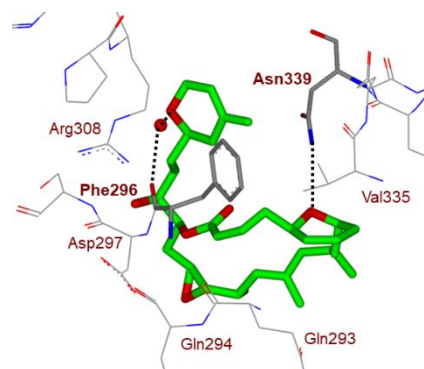


Figure 4. Structure of laulimalide (**4**, green carbons)-bound to β -tubulin. Hydrogen bonds with THP oxygens are shown with dotted lines.

Also, the oxygen atoms of the dihydropyran side chain form a water-mediated hydrogen bond to the side chain OH of Tyr312 and the main chain backbone carboxyl oxygen of Phe296. These interactions are likely very important for laulimalide's potent anticancer activity. Similarly, X-ray structural studies of platensimycin (**6**)-bound bacterial enzyme beta-ketoacyl synthase II (FabF) show that the tetrahydropyranyl oxygen is involved in hydrogen bonding interactions with the Thr270 residue.⁴⁸ Interestingly, the desoxy derivative showed significantly reduced activity, demonstrating the importance of the ring oxygen.⁵¹

The cyclic ether templates, basically may be viewed as peptidomimetic scaffolds. We therefore speculated that incorporation of similar cyclic ether templates in our design of HIV-1 protease inhibitors may lead to nonpeptide derivatives which would alleviate problems inherent to peptide or peptidomimetic based first generation protease inhibitor drugs.^{52,53} We first systematically explored a variety of cyclic ethers and cyclic sulfone-derived conformationally constrained structural templates to replace peptide-like amide bonds. We then demonstrated that cyclic ether or sulfone-derived heterocycles can mimic peptide and amide bond interactions in the HIV-1 protease active site. This led to the design of a range of highly potent and nonpeptide HIV-1 protease inhibitors with cyclic ether structural features.^{16,17,27} Our further design optimization then focused on promoting hydrogen bonding interactions with the backbone atoms in the S2 to S2' subsites of HIV-1 protease.^{29,34} These design and optimization efforts ultimately culminated the discovery and development of darunavir.^{18,20,28} In the following section, we briefly highlight the

chronology of these design events that led to the development of darunavir; the first approved treatment for patients with drug-resistant HIV.

Design of Cyclic Ether Containing HIV-1 Protease Inhibitors: From Saquinavir to Darunavir

Saquinavir (**8**, R031-8959) is one of the first HIV-1 protease inhibitor drugs that was approved by the FDA in 1996 for treatment of patients with HIV/AIDS.^{54,55} Subsequently, a number of other first-generation inhibitor drugs were approved for use in combination therapy with reverse transcriptase inhibitor drugs.^{19,56,57} These combination therapies with HIV-1 protease inhibitors resulted in a dramatic reduction of HIV/AIDS related deaths among patients who had access to these therapies.^{9,10} However, therapeutic efficacy of first-generation PI drugs was limited due to peptide-like features and poor ADME properties of these drugs. The emergence of drug-resistant HIV-1 strains made the therapies ineffective. Subsequent development addressing these issues led to second-generation PI drugs, such as lopinavir, atazanavir, and tipranavir.^{37,56} However, the emergence of highly multidrug-resistant HIV-1 variants among infected patients became a significant limitation.

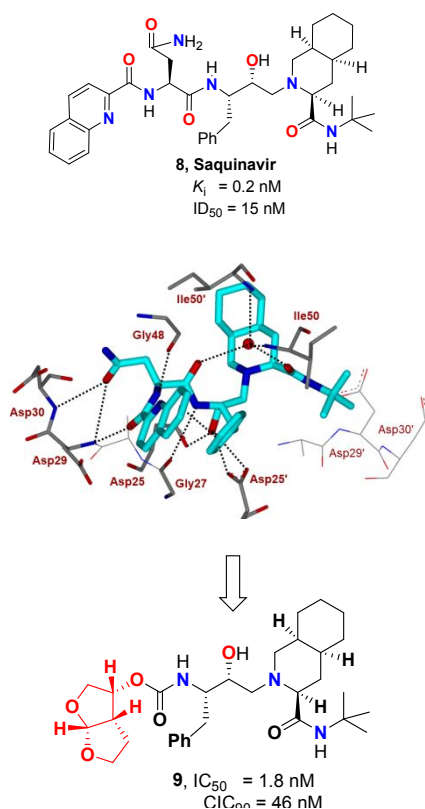


Figure 5. Structure and activity of inhibitors **8** and **9** (PDB: 1HXB).

In our effort to utilize structure-based design to develop next generation nonpeptide PIs effective against drug-resistant HIV-1 variants, we first explored saquinavir active site interactions with a stereochemically-defined cyclic ether and cyclic sulfone-derived heterocycles in an effort to replace the peptidic bonds of saquinavir. These endeavors resulted in the design and discovery of a variety of potent nonpeptide PIs.⁵⁸⁻⁶¹ Further optimization of cyclic ether templates followed based upon the X-ray structures of saquinavir-bound HIV-1 protease and X-ray structures of early lead inhibitors with HIV-1 protease. The saquinavir-bound HIV-1 protease X-ray structure revealed that the carboxyl oxygen of the P2-asparagine ligand and the amide carboxyl oxygen of P3-quinaldic amide form two strong hydrogen bonds with the backbone amide NHs of Asp30 and Asp29 in the S2 and S3 subsites (Figure 5).^{54,62} Based upon the X-ray structures, we then designed a fused bicyclic hexahydrofuro[2,3-*b*]furan to replace both amide carbonyl bonds in the saquinavir structure.^{27,61,62} As shown in Figure 4, inhibitor **9**, with a stereochemically defined (3*R*,3*aS*,6*aR*)-*bis*-tetrahydrofuranlyl urethane displayed very potent HIV-1 protease inhibitory activity as well as antiviral activity. Indeed, our X-ray structural studies of PI-**9**-bound HIV-1 protease and comparison of X-ray structure of saquinavir-bound protease revealed that the fused cyclic ether template of the *bis*-THF ligand oxygens formed strong hydrogen bonds with Asp29 and Asp30 backbone amide NHs in the active site.^{61,62} The bicyclic *bis*-THF core also makes extensive van der Waals interactions in the S2 subsite. In essence, the *bis*-THF ligand effectively replaced two amide bonds and the bulky P3-10π-aromatic quinaldic moiety of saquinavir. Through our detailed structure-activity relationship studies, we also demonstrated that ring stereochemistry, position of ring oxygens, ring size of *bis*-THF in PI9, are optimal for effective binding interactions in the active site.^{27,61}

Following our discovery of the cyclic ether derived nonpeptide *bis*-THF heterocycle as a highly effective P2 ligand for HIV-1 protease inhibitors, we then focused our efforts to design PIs that would make extensive backbone hydrogen bonding interactions in both S2 to S2' subsites.^{29,34} Since the active enzyme, HIV-1 protease is a homodimer, we also planned

Table 1. Inhibitory potency of **10** against wild-type and mutant proteases

Enzyme	K_i (pM)	$K_{i,wt}/K_{i,mut}$	Vitality ^a
WT	14	1	1
D30N	<5	0.33	0.3
V32I	8	0.57	0.5
I84V	40	2.85	1
V32I/I84V	70	5	0.7
M46F/V82A	<5	0.33	0.1
G48V/L90M	<5	0.33	0.1
V82F/I84V	7	0.5	0.1
V82T/I84V	22	1.57	0.1
V32I/K45I/F53L/A71V/I84V/L89M	31	2.2	0.1
V32I/L33F/K45I/F53L/A71V/I84V	46	3.3	0.1
20R/36I/54V/71V/82T	31	2.2	0.1

^aThe vitality is a measure of the enzymatic fitness of a mutant protease in presence of an inhibitor, here **10** (determined as $(K_i^*k_{cat}/K_m)_{mut}/(K_i^*k_{cat}/K_m)_{wild}$).

to promote extensive van der Waals interactions throughout the active site. Towards these objectives, we first designed PIs incorporating (*R*)-(hydroxyethyl)sulfonamide-derived transition-state binder with a *p*-methoxybenzene sulfonamide as the P2' ligand, with the plan to have hydrogen binding interactions in the S2'-site through the methoxyl oxygen.^{62,63} This optimization resulted in PI **10** (Figure 6, later named as TMC-126), which exhibited exceptional HIV-1 protease inhibitory activity as well as antiviral activity. Enzyme inhibitory activity of inhibitor **10** against mutant proteases resistant to a majority of first-generation approved PIs is shown in Table 1.^{64,65} As can be seen, protease inhibitory activity of **10** is less than 100 pM and changes of activity were not more than 5-fold. Table 2 shows antiviral activity of inhibitor **10** against a panel of highly multi-PI-resistant HIV-1 strains isolated from patients. Antiviral activity of PI **10** did not change much against these multidrug-resistant HIV-1 variants whereas, other

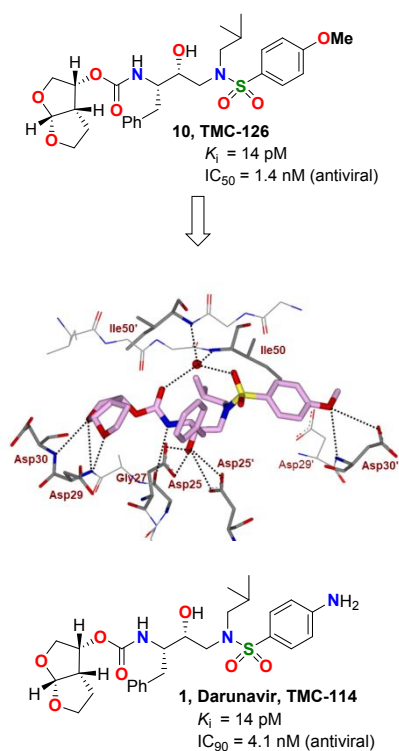


Figure 6. Structure and activity of inhibitors **1** and **10**. X-ray structure of **10**-bound HIV-1 protease (PDB: 317E).

approved PIs exhibited a high level of drug resistance.^{63,66} The X-ray structural analysis of **10**-bound HIV-1 protease revealed that both the *bis*-THF ligand and the 4-methoxy sulfonamide P2'-ligand formed extensive hydrogen bonding and van der Waals interactions with the backbone atoms in the S2 and S2' subsites.^{32,37,67} As shown in Figure 6, both lone pairs of top tetrahydrofuran oxygen atom of *bis*-THF ligand form two hydrogen bonds with Asp30 and Asp29 backbone amide NHs. The bottom oxygen however forms a single hydrogen bond with Asp29 backbone amide NH in the S2 subsite. Also, both P1 and P1' ligands fill in the hydrophobic S1 and S1' subsites effectively.

Inhibitor **10** showed a high genetic barrier to drug resistance acquisition. Also, *in vitro* selection of HIV-1 strains resistant to inhibitor **10** was difficult to attain.⁶⁶ The extraordinary antiviral activities of **10** against multidrug-resistant HIV-variants as well as its durability towards the development of drug-resistance can be attributed to the extensive interactions of **10** with the protease, particularly the formation of a network of hydrogen bonding interactions with the backbone atoms from the S2 to S2'-subsites.^{29,34}

Table 2. Antiviral activity of **10** against HIV-1 isolated from previously treated HIV-infected patients

Virus ^[a]	$IC_{50} \mu\text{M}$ (fold change)					
	RTV	IDV	SQV	NFV	APV	10
WT	0.044 (1)	0.013 (1)	0.010 (1)	0.023 (1)	0.025 (1)	0.0007 (1)
1	>1 (>23)	>1 (>77)	0.27 (27)	>1 (>43)	0.27 (11)	0.004 (6)
2	>1 (>23)	0.49 (38)	0.037 (4)	0.33 (14)	0.28 (11)	0.0013 (2)
3	>1 (>23)	0.49 (38)	0.036 (4)	>1 (>43)	0.26 (10)	0.001 (1)
4	>1 (>23)	0.21 (16)	0.033 (3)	0.09 (4)	0.31 (12)	0.0016 (2)
5	>1 (>23)	>1 (>77)	0.31 (31)	0.41 (18)	0.67 (27)	0.0024 (3)
6	>1 (>23)	0.30 (23)	0.19 (19)	>1 (>43)	0.16 (6)	0.0005 (1)
7	>1 (>23)	>1 (>77)	0.12 (12)	>1 (>43)	0.49 (20)	0.0055 (8)
8	>1 (>23)	0.55 (42)	0.042 (4)	>1 (>43)	0.15 (6)	0.001 (1)

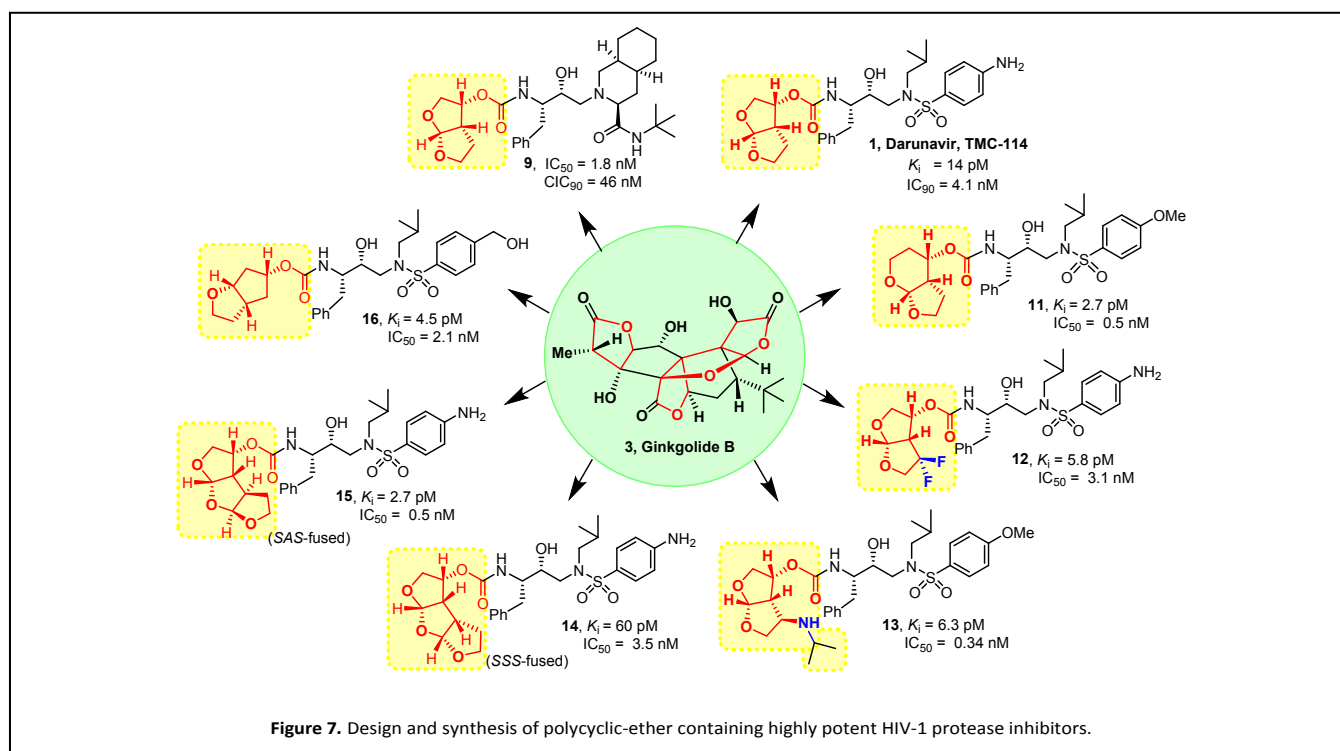
^[a] Amino acid substitutions identified in the protease-encoding regions of viruses compared to the consensus sequence cited from the Los Alamos database. See reference 57 for details.

We have designed and synthesized a variety of other very potent PIs that promote the formation of a network of hydrogen bonds like PI **10**. Further optimization of ligand binding as well as pharmacokinetic properties ultimately led to the design and development of inhibitor **1** (Darunavir, TMC-114) with a *bis*-THF P2 ligand and a 4-aminobenzenesulfonamide as the P2' ligand. Darunavir exhibited exceptionally potent protease inhibitory and antiviral activity.^{28,62,63} Also, it displayed unprecedented broad-spectrum antiviral activity against a wide range of highly multidrug-resistant HIV-1 variants.^{21,22} As shown in Table 3, darunavir exhibited very potent antiviral activity ($IC_{50} = 0.003\text{-}0.029 \mu\text{M}$) against a series of HIV-1 strains, which were selected for their resistance against saquinavir (SQV), amprenavir (APV), indinavir (IDV), nelfinavir (NFV), and ritonavir (RTV) after exposure of the virus to increasing concentrations of these PIs. Also, darunavir maintained excellent antiviral activity

Table 3. Activity of darunavir against HIV-1 clinical isolates in PHA-PBMC infected cells^[a]

Virus	IC_{50} values (μM)					
	SQV	APV	IDV	NFV	RTV	DRV (1)
WT	0.010	0.023	0.018	0.019	0.027	0.003
1	0.004	0.011	0.018	0.033	0.032	0.003
2	0.23 (23)	0.39	>1 (>56)	0.54 (28)	>1 (>37)	0.004 (1)
3	0.30 (30)	0.34	>1 (>56)	>1 (>53)	>1 (>37)	0.02 (7)
4	0.35 (35)	0.75 (33)	>1 (>56)	>1 (>53)	>1 (>37)	0.029 (10)
5	0.14 (14)	0.16 (7)	>1 (>56)	0.36 (19)	>1 (>37)	0.004 (1)
6	0.31 (31)	0.34 (15)	>1 (>56)	>1 (>53)	>1 (>37)	0.013 (4)
7	0.037 (4)	0.28 (12)	>1 (>56)	0.44 (23)	>1 (>37)	0.003 (1)
9	0.029 (3)	0.25 (11)	0.39 (22)	0.32 (17)	0.44 (16)	0.004 (1)

formed two very strong hydrogen bonds with the Asp29 and



^[a] Amino acid substitutions identified in the protease-encoding regions of viruses compared to the consensus sequence cited from the Los Alamos database. See reference 13 for details.

against a panel of highly multi-PI-resistant HIV-1 variants isolated from AIDS patients who previously failed anti-HIV regimens after receiving other anti-HIV drugs.^{21,22} Darunavir received an accelerated FDA approval in June, 2006, for patients harboring drug-resistant HIV. Then in 2008, its approval was extended to all HIV/AIDS patients including pediatrics.¹⁶ Darunavir emerged as a first-line therapy and it is often preferred for HIV/AIDS patients who did not receive antiretroviral drugs previously due to its tolerance and a high genetic barrier to the development of drug-resistant viruses compared to other HIV-1 protease inhibitor drugs.^{15,16} The unique structural design of darunavir, its molecular interactions with the protease active site, and resilience against multidrug-resistant HIV-1 variants have stimulated significant research interest regarding its mechanism of action.^{28,68} Using intermolecular fluorescence resonance energy transfer (FRET)-based HIV expression assay, we have shown that darunavir blocks HIV-1 protease dimerization.^{69,70} Therefore, darunavir's unique dual modes of action which include (1) inhibition of the catalytic protease dimer and (2) inhibition of protease monomer dimerization to form the active enzyme, may be responsible for its robust drug-resistance profiles and high genetic barrier to the development of drug-resistant HIV-1 variants.^{20,28,68}

We have determined a high resolution X-ray crystal structure of darunavir-bound HIV-1 protease (Figure 1). These structures show that darunavir makes extensive interactions including a network of hydrogen bonds throughout the HIV-1 protease active site. Both oxygens of the P2 *bis*-THF ligand

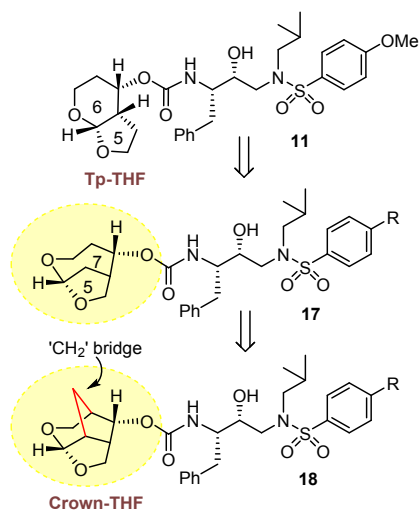
Asp30 backbone amide NHs in the S2 subsite.^{30,31,71} The P2'-aminosulfonamide's amine functionality formed hydrogen bonds with the Asp30' backbone NH as well as with the side chain carboxylic acid in the S2'-subsite. Both P1 phenylmethyl group and the P1' isobutyl moiety filled in the hydrophobic pockets in S1 and S1' subsites. Furthermore, a tetra-coordinated structural water molecule forms hydrogen bonds with both NH atoms of flap residues Ile50/50' and the inhibitor's P2 urethane carbonyl and one of the P2'-sulfonamide (SO₂) oxygens.^{72,73} Presumably, these ligand-binding site interactions are responsible for darunavir's unprecedented antiviral activity and drug-resistance profiles.^{29,34}

Following darunavir's development, utilizing our SAR and critical molecular insights from active site interactions, we have designed a variety of other bicyclic and polycyclic ether templates to enhance the backbone-binding interactions, as well as to improve van der Waals interactions in the active site. These endeavours resulted in a series of exceptionally potent HIV-1 protease inhibitors that exhibited improved antiviral activity against multidrug-resistant HIV-1 variants compared to darunavir and other approved PI drugs. Figure 7 depicts structure and potency of a selected number of representative inhibitors (**11-16**).⁷⁴⁻⁸¹ A detailed account of their design, synthesis, biological evaluation and structural studies have been reported and reviewed by us.¹⁹ Of particular importance, we designed and incorporated stereochemically defined and conformationally constrained cyclic-ether structural features in the P2 ligand to interact specifically with active site.

Design of Crown-THF-based New Generation of HIV-1 Protease Inhibitors

In our post darunavir development, we set out to design a structurally more conformationally constrained and preorganized ligand that would enhance overall backbone hydrogen bonding and van der Waals interactions in the protease active site.^{29,34} The X-ray structure of darunavir-bound HIV-1 protease revealed that the *bis*-THF P2 ligand can be modified to enhance ligand-binding site interactions.^{30,31} In the context of our design of bicyclic 6-5-fused acetal-derived inhibitor **11**, we showed that the hexahydrofurofuran heterocycle has made better alignment with the backbone amide NHs in the S2-subsite over the *bis*-THF ligand.⁷⁴ Presumably, the extra methylene group in the new tetrahydropyranyl tetrahydrofuran-fused (Tp-THF) ligand may have contributed toward improved van der Waals interactions. Inhibitor **11** displayed enhanced enzyme inhibitory and antiviral activity over the corresponding *bis*-THF-derived inhibitor **10**. In addition, inhibitor **11** exhibited impressive antiviral activity against a panel of highly multidrug-resistant HIV-1 variants, comparable to darunavir and its methoxy derivative **10**.^{74,82} Indeed, our X-ray structural analysis of **11**-bound HIV-1 protease and **10**-bound HIV-1 protease complexes show that both oxygens of the Tp-THF ligand of inhibitor **11** promoted stronger hydrogen bond formation with the backbone NHs of Asp29 and Asp30.⁷⁴

Based upon the above critical ligand-binding site interactions, we then speculated that a bicyclic 7-5-fused acetal-derived P2 ligand in inhibitor structure **17** (Figure 8) may further improve hydrogen bonding interactions in the active site, however, due to conformational instability of the seven-membered ring cycle, we planned to incorporate a methylene bridge to further stabilize the conformation. This hypothesis led to the design of a conformationally restricted crown-like tetrahydropyrano-tetrahydrofuran (crown-THF or *Crn*-THF) ligand shown in inhibitor structure **18**. The ligand has three extra methylene groups compared to *bis*-THF ligand in darunavir and three methylene groups are expected to engage in van der Waals interactions with nearby residues in the active site. This *Crn*-THF ligand is a relatively larger P2 ligand than the *bis*-THF ligand of darunavir, and we speculated that it may confer better adaptability to protease mutation.



This journal is © The Royal Society of Chemistry 20xx

Figure 8. Design of Crown-THF P2 ligand

Our examination of the preliminary models of *endo*-*crn*-THF and *exo*-*crn*-THF-derived inhibitors indicated that the acetal oxygens in the *endo*-derivative are more favorably positioned to form hydrogen bonds with Asp30 and Asp29 amide NHs. The tricyclic core of *endo*-*crn*-THF ligand also appeared to fill the hydrophobic pocket in the S2 site more effectively than the *exo* isomer. As can be seen in Figure 9, inhibitor **19** with an *endo*-*Crn*-THF P2 ligand and a 4-methoxybenzenesulfonamide as the P2'-ligand, displayed an enzyme inhibitory K_i of 14 pM compared to inhibitor **20** with an *exo*-*crn*-THF ligand (K_i 10.8 nM).^{83,84} Inhibitor **21**, with a *p*-aminobenzenesulfonamide as the P2'-ligand, exhibited a comparable K_i value to compound **19**. Both inhibitors **19** and **21** with an *endo*-*crn*-THF P2 ligand exhibited very potent antiviral activity comparable to darunavir and inhibitor **10**. Inhibitor **20** with an *exo*-*crn*-THF displayed no measurable antiviral activity.

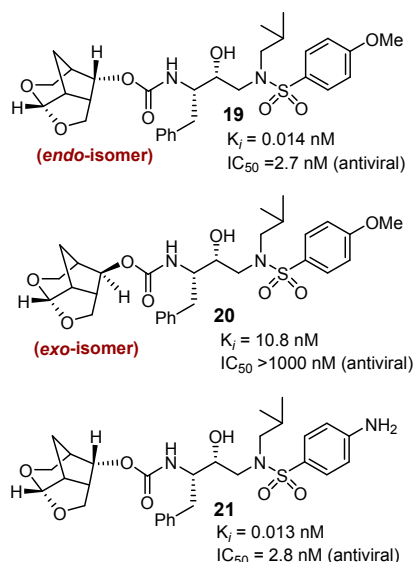


Figure 9. Structure and activity of inhibitor 19-21.

We determined a high resolution X-ray crystal structure of inhibitor **19**-bound HIV-1 protease.^{83,85} As shown in Figure 10, both acetal oxygens of the tricyclic crown scaffold interact with backbone residues and the side chain Asp30 carboxylate group in S2 subsite, comparable to the interactions of darunavir. This *Crn*-THF ligand is conformationally restricted and larger than the P2 *bis*-THF ligand of darunavir. It displaced residues 45'-48'

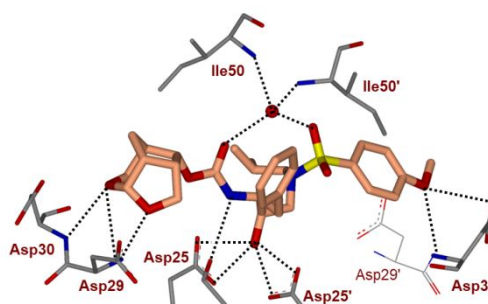


Figure 10. Inhibitor **19**-bound X-ray structure of HIV-1 protease (PDB code: 5ULT). All hydrogen bonds are indicated by dotted lines.

by up to 0.8 Å, and resulted in an enlarged inhibitor-binding cavity. The *Crn*-THF ligand is also involved in significantly enhanced van der Waals interactions with Ile47, Val32, and Leu76 residues in the S2-site compared to *bis*-THF ligand of darunavir.

For improving overall ligand-binding interactions of inhibitors, we then planned to replace P2'-ligand aminobenzene

Table 4. Antiviral activity of inhibitors **2** and **22** against highly DRV-resistant HIV-1 variants.

	Mean IC ₅₀ in nM ± SD (fold-change)				
	LPV	ATV	DRV	22 (GRL-121)	2 (GRL-142)
^c HIV _{NL4-3} ^{WT}	13	4.0	3.2	0.26	0.019
HIV _{DRV^RP20}	>1000 (>77)	450 (113)	51 (16)	0.075 (0.3)	0.0024 (0.1)
HIV _{DRV^RP30}	>1000 (>77)	>1000 (>250)	220 (79)	1.9 (7)	0.023 (1)
HIV _{DRV^RP51}	>1000 (>77)	>1000 (>250)	2500 (781)	32 (279)	1.2 (63)

Numbers in parentheses represent fold changes in IC₅₀s for each isolate compared to the IC₅₀s for wild-type cHIV_{NL4-3}^{WT}. All assays were conducted in triplicate, and the data shown represent mean values (±1 standard deviation) derived from the results of three independent experiments.

sulfonamide ligand of darunavir with other aromatic heterocycles that would promote enhanced hydrogen bonding interactions as well as to improve hydrophobic contacts in the S2' subsite. In particular, we planned to incorporate various alkylaminobenzothiazole and benzoxazole heterocycles in combination with the crown-THF P2 ligand for this new class of HIV-1 protease inhibitors. We selected these heterocycles as they are structural features of numerous medicinally important compounds with drug-like properties.^{86,87} Among various

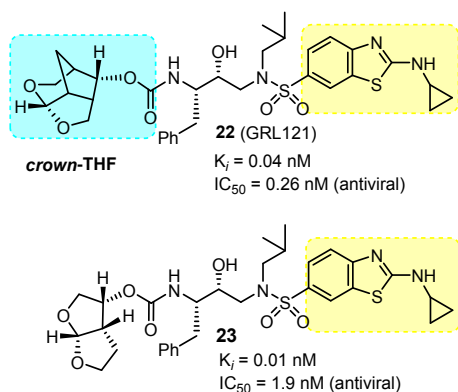


Figure 11. Structure and activity of inhibitor **22-23**.

alkylamino groups examined by us, aminocyclopropylbenzothiazole (Abt) sulfonamide as the P2' ligand showed the optimum results. As shown in Figure 11, replacement of the 4-aminosulfonamide P2' ligand of inhibitor **21**, with an aminocyclopropylbenzothiazole ligand, resulted in inhibitor **22**,

which displayed a slight reduction of enzyme K_i value, however there is a nearly 10-fold improvement of antiviral activity over inhibitor **21**.⁸³ In comparison, inhibitor **23** resulting from substitution of darunavir's 4-aminosulfonamide P2' ligand with an aminocyclopropylbenzothiazole ligand showed only slight improvement in antiviral activity over darunavir. Inhibitors **21**, **22** and **23** were evaluated against DRV-resistant HIV-1 variants. Inhibitor **22** exhibited very potent antiviral activity against all HIV-1 variants examined compared to inhibitors **21**, **23**, and several FDA approved PI drugs.^{83,84}

We determined the X-ray crystal structure of inhibitor **22**-bound wild-type HIV-1 protease and the important interactions are shown in Figure 12. In particular, the P2' ligand's benzothiazole amine nitrogen also makes strong hydrogen bonds with the backbone NH of Asp30' and the cyclopropyl amine nitrogen forms an additional hydrogen bond with the side chain carboxylate of Asp30'. The Abt ligand makes more hydrophobic contacts with the protease than the 4-aminobenzenesulfonamide ligand of DRV. Also, both oxygens of the *crn*-THF ligand formed strong hydrogen bonds with backbone amide NHs of Asp29 and Asp30. The tricyclic ligand scaffold is involved in van der Waals interactions with the HIV-1 protease.⁸³ Presumably, these extensive molecular interactions are responsible for observed superior antiviral profiles of inhibitor **22** against a panel of highly multidrug-resistant HIV-1 variants.^{83,84}

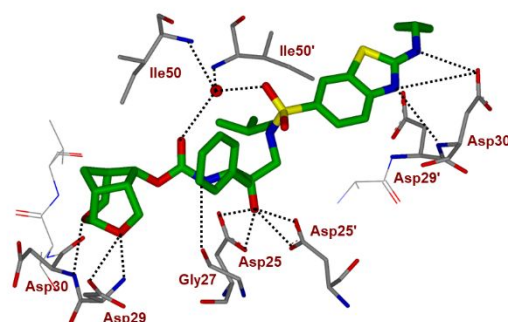


Figure 12. Inhibitor **22**-bound X-ray structure of HIV-1 protease (PDB code: 5TYR). All hydrogen bonds are indicated by dotted lines.

Based upon our detailed structural analysis of inhibitor **22**-bound HIV-1 protease, we then planned to further optimize the inhibitor-protease van der Waals hydrogen ligand-binding site interactions of inhibitor **22** to improve drug properties. Our overall plans were to preserve all backbone bonding interactions of **22** with HIV-1 protease and interactions in the active site. We planned to incorporate fluorine atoms in the P1-ligand to improve van der Waals contact in the S1-subsite. Our particular preference for fluorine atoms is due to fact that fluorines are often used to increase lipophilicity and help improve drug penetration in the CNS.^{88,89} As shown in Figure 13, our incorporation of a 3,5-difluorobenzyl moiety as the P1 ligand in **22** resulted in exceptionally potent inhibitor **2**, displaying a protease inhibitory K_i value of 14 pM and antiviral IC₅₀ value of 0.017 nM, a more than 150-fold potency

Table 5. Antiviral activity of **2** and **22** against highly PI-resistant HIV-1 variants.
Mean IC₅₀ in nM ± SD (fold-change)

Virus Species	LPV	ATV	DRV	22 (GRL-121)	2 (GRL-142)	
Wild-type	^c HIV _{NL4-3} ^{WT}	13 ± 2	4.0 ± 2.3	3.2 ± 0.7	0.26 ± 0.05	0.019 ± 0.017
<i>in vitro</i> HIV _{PI} ^{R*}	HIV _{SQV-52M}	>1000 (>77)	430 ± 20 (108)	17 ± 7 (5)	0.026 ± 0.01 (0.1)	0.00018 ± 0.00003 (0.009)
	HIV _{APV-52M}	280 ± 15 (22)	3.0 ± 1.0 (1)	39 ± 16 (12)	0.13 ± 0.08 (0.5)	0.000085 ± 0.000008 (0.0004)
	HIV _{LPV-52M}	>1000 (>77)	46 ± 10 (12)	280 ± 50 (86)	0.0018 ± 0.001 (0.007)	0.000019 ± 0.0000014 (0.0001)
	HIV _{DV-52M}	250 ± 15 (19)	56 ± 9 (14)	37 ± 8 (12)	0.0092 ± 0.016 (0.04)	0.00018 ± 0.00028 (0.009)
	HIV _{NFV-52M}	37 ± 3 (3)	12 ± 2 (3)	7.7 ± 3 (2)	0.048 ± 0.02 (0.2)	0.00024 ± 0.00026 (0.01)
	HIV _{ATV-52M}	310 ± 20 (24)	>1000 (>250)	25 ± 1 (8)	0.092 ± 0.09 (0.4)	0.015 ± 0.004 (0.8)
	HIV _{TPV-152M}	>1000 (>77)	>1000 (>250)	40 ± 3 (13)	0.063 ± 0.02 (0.2)	0.00024 ± 0.00007 (0.01)

**in vitro* HIV_{PI}^R, *in vitro* PI-selected HIV-1 variants; **_{rCL}HIV, recombinant clinical HIV-1 variants. Numbers in parentheses represent fold changes in IC₅₀s for each isolate compared to the IC₅₀s for wild-type ^cHIV_{NL4-3}^{WT}. All assays were conducted in triplicate, and the data shown represent mean values (±1 standard deviation) derived from the results of three independent experiments. DOI: <https://doi.org/10.7554/eLife.28020.005>

enhancement over darunavir. Inhibitor **2** is over 15-fold more potent than inhibitor **22** with no fluorine, showing the importance of *bis*-fluorines on the P1-ligand.^{90,91} We also investigated activity of monofluoro derivatives. Inhibitor **24** with a 3-fluorophenylmethyl as the P1-ligand displayed a protease inhibitory K_i value of 0.3 pM and an antiviral IC₅₀ of 0.055 nM. Inhibitor **25** with a 4-fluorophenylmethyl as the P1 ligand exhibited a reduction in both protease inhibitory and antiviral activity over its 3-fluoro derivative.^{90,92} We also investigated various alkylaminobenzoxazole derivatives as the P2' ligand in place of P2' ligand of inhibitor **2**. Inhibitor **26** with an isopropylaminobenzoxazole displayed the best results, showing a K_i value 5 pM and antiviral IC₅₀ of 0.055 nM.⁹³

We evaluated inhibitor **2** and inhibitor **22** without fluorine against darunavir-resistant HIV-1 variants and compared antiviral IC₅₀ values against approved PIs. These DRV-resistant variants HIV-1_{DRV}^Rs are highly resistant to clinically used PIs including DRV and RT inhibitors (NRTIs) such as tenofovir. As shown in Table 4, both LPV and ATV failed to block the replication of DRV-resistant HIV-1 variants. Inhibitor **22** with no fluorine very effectively blocked the replication of all three highly DRV-resistant HIV-1 variants.^{90,91} However, inhibitor **2** with two-fluorines on the P1 ligand displayed exceptional antiviral activity in low picomolar concentration against DRV-resistant HIV-1 variants selected in the presence of DRV over 20

viral passages.^{94,95} Inhibitor **2** maintained IC₅₀ values of 1.2 nM against HIV-1_{DRV}^{R51}, the most multi-PI/NRTI-resistant HIV-1 variants. In comparison, darunavir displayed >1000-fold increase in its IC₅₀ values (IC₅₀ 2.5 μM). Furthermore, inhibitor **2** exerted very potent antiviral activity against the HIV-2 variants and showed much improved cytotoxicity profile with a selectivity index (CC₅₀/IC₅₀) as high as 2,473,684 compared to DRV (41,562).^{90,91}

Inhibitor **22** was then evaluated against a variety of HIV-1 variants that had been selected *in vitro* with other FDA-approved PI drugs. These variants acquired multiple amino acid substitutions in the protease of the virus resulting in viral resistance to each PI drug. As shown in Table 5, two widely used PIs LPV and ATV failed to block these variants effectively compared to DRV. Inhibitor **22** without fluorine, maintained very potent antiviral activity against all resistant HIV-1 variants (IC₅₀ values ranging from 1.8 pM to 0.13 nM). Inhibitor **2** with *bis*-fluorines displayed exceptional antiviral activity against all seven highly P1-resistant HIV-1 variants, showing antiviral IC₅₀ values, ranging from 8.5 fM to 0.015 nM.^{90,91}

We assessed genetic barrier to the emergence of HIV-1 variants resistant to inhibitors **2** and **22** and compared with other approved PI drugs. We aimed to select HIV-1 variants resistant to ATV and DRV and inhibitors **2** and **22** by propagating ^cHIV_{NL4-3}^{WT} using increasing concentrations of each inhibitor. As shown in Figure 14 (top panel), HIV-1 became resistant to ATV and started replicating in the presence of 5 μM by week 36. There were 7-amino acid substitutions in the protease encoding region.⁹¹ However, the emergence of DRV-resistant variants were considerably delayed at concentration above 0.1 μM DRV at week 36. In comparison, ^cHIV_{NL4-3}^{WT} failed to spread in the presence of 0.01 μM concentration of **22** or in the presence of 0.003 μM concentrations of **2**, even after 36 weeks, indicating that HIV-1 failed to select any meaningful substitutions in the PR encoding region of the virus. The effect of inhibitors **2** and **22** against a mixture of 11 multi-PI-resistant clinical HIV-1 isolates (HIV_{11MIX}) were also evaluated and the results are shown in Figure 14 (bottom panel). As can be seen, the virus quickly became highly resistant to both ATV and DRV however, both inhibitors **2** and **22** very effectively blocked the propagation of HIV_{11MIX} in the presence of >0.07 nM inhibitor **22** or >0.017 nM concentration of inhibitor **2**. The results indicate

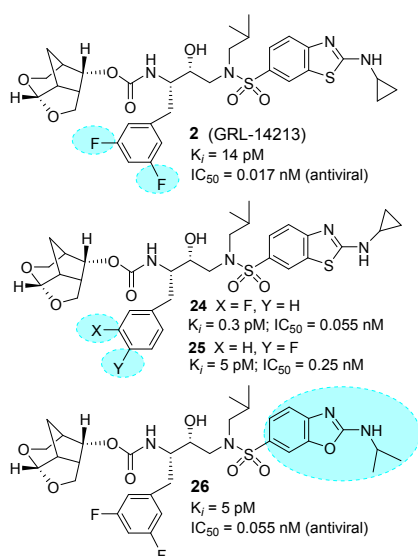


Figure 13. Structure and activity of inhibitors **2** and **24-26**.

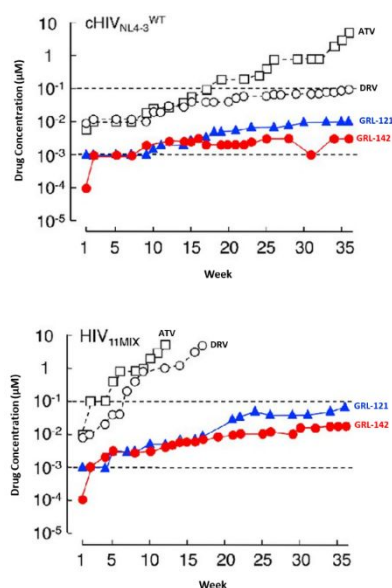


Figure 14. Inhibitor **2** shows high genetic barrier to the development of HIV-1 variants *in vitro*. Top panel A, against HIV_{NL4-3}; bottom panel B, against a mixture of 11 multi-PI-resistant HIV-1 isolates (HIV_{11MIX}). DOI: <https://doi.org/10.7554/eLife.28020.005>

that inhibitor **2** displayed an extremely high genetic barrier to resistance.⁹¹

It appears that inhibitor **2**, like DRV, exhibits a dual mechanism of action, (i) inhibition of HIV-1 protease dimerization and (ii) inhibition of proteolytic activity of HIV-1 protease. Dimerization of HIV-1 protease subunits is an essential process for the acquisition of proteolytic activity of HIV-1 protease. We previously demonstrated that DRV and TPV inhibit the dimerization of HIV-1 protease monomers by using the FRET-based HIV-1 expression assay.^{69,70} Other approved PIs do not block dimerization of HIV-1 protease subunits. We have now observed that inhibitor **2** blocks protease dimerization very potently, at 0.1 nM concentration, which were significantly lower than DRV. It improved by at least a factor of 1000-fold (thousand) compared to DRV.⁹¹ The data suggests that inhibitor **2** could be developed as a monotherapy.

Inhibitor **2** is more lipophilic than inhibitor **22** or DRV. Inhibitor **2** shows favorable penetration into the brain of rats. When DRV and compound **2** were perorally administered to rats ($n = 2$) at a dose of 5 mg/kg plus RTV (8.33 mg/kg), the C_{max} was achieved around 90 and 360 min after the administration, respectively. The concentrations of DRV and inhibitor **2** in plasma, CSF, and brain were determined in 15 and 90 min for DRV and 60 and 360 min for inhibitor **2** after the administration. Drug concentrations of **2** in the brain were 7.24 ± 9.65 and 32.6 ± 1.4 nM in 60 and 360 min, respectively. The latter concentration (32.6 nM) represents $\sim 1,882$ fold greater than the IC₅₀ value and ~ 114 fold greater than the IC₉₅ value of inhibitor **2**. The data strongly suggest that inhibitor **2** would potently block the infection and replication of HIV-1 in the brain.^{90,91} This may serve to prevent or treat HAND complication.

We determined a high resolution X-ray crystal structure of inhibitor **2**-bound wild-type HIV-1 protease and the important interactions are shown in Figure 14. Inhibitor **2** retains all key hydrogen bonds observed between DRV and the backbone atoms of HIV-1 protease. The P2' thiazole nitrogen of **2** forms a hydrogen bond interaction with the backbone amide of Asp 30' similar to the interaction of 4-aminobenzene of DRV. The P2' amino group forms a strong hydrogen bond interaction with the Asp 30' side chain. Interestingly, the cyclopropyl group bulges out and forms N-H...O interactions with the side chain of Asp 30'. Both oxygen atoms in the *Cmn*-THF form strong hydrogen bonds with the backbone amide NHs of Asp29 and Asp30. In addition, the *Cmn*-THF ligand has formed enhanced van der Waals interactions in the S2 subsite compared to the *bis*-THF ligand of darunavir.^{90,91}

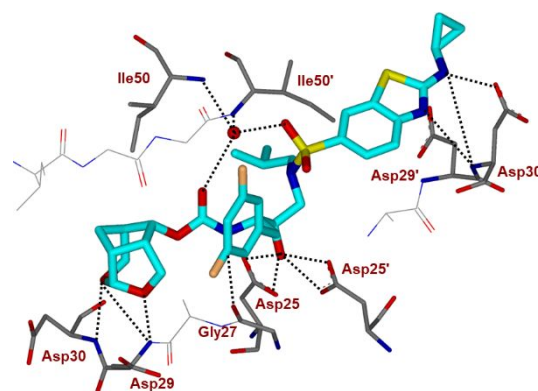


Figure 15. Inhibitor **2**-bound X-ray structure of HIV-1 protease. The major orientation of the inhibitor is shown. The inhibitor carbon atoms are shown in green, water molecules are red spheres, and the hydrogen bonds are indicated by dotted lines (PDB ID: 6BZ2).

As shown in Figure 16, both fluorine atoms on the P1 ligand of inhibitor **2** form important halogen bond interactions in the protease active site. One of the fluorine atoms interacts with the tips of both flaps by forming a strong polar interaction with the backbone NH group of Ile50 (C-F...H-N) and an orthogonal multipolar interaction (C-F...C-O) with the backbone carbonyl of Gly49.^[41,42] This fluorine makes hydrophobic interactions with Gly48, Ile50 and Pro81'. The second fluorine atom forms multipolar interactions with the guanidium group of Arg8', stabilizing the dimer of HIV-1 protease by a critical inter-subunit ion pair. This fluorine atom also has van der Waals contact with Val82'. Both P1 and P2' ligands in inhibitor **2** considerably contributed additional interactions, improving the favorable inhibitor-HIV-1 protease interactions in comparison to DRV. These new ligand-binding site interactions are likely to account for the improved activity of inhibitor **2**.

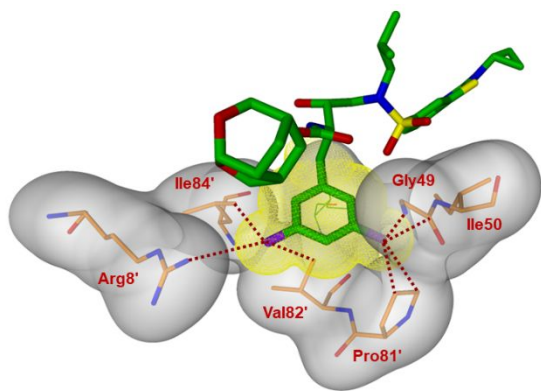
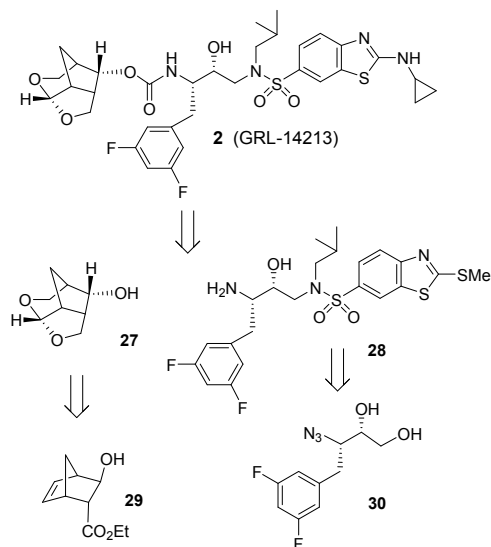


Figure 16. Side view of the S1 subsite. The protein surface is shown in transparent gray. The van der Waals surface for the fluorinated P1-ligand for inhibitor **2** is shown in orange wire mesh and van der Waals contacts are shown by dotted lines.

Synthesis of Crown-THF-derived HIV-1 Protease Inhibitor **2** (GRL-142)

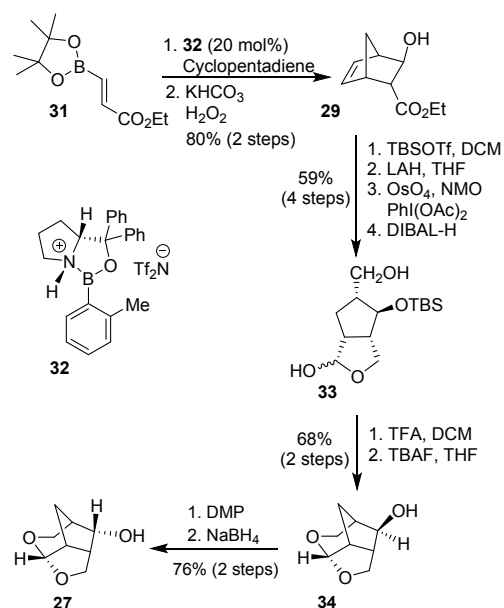
Our synthetic strategy for inhibitor **2** is shown in Scheme 1. Inhibitor **2** was obtained by alkoxy-carbonylation of ligand alcohol **27** and hydroxyethylaminosulfonamide amine derivative **28**.^{96,97} Stereochemically defined tricyclic ligand alcohol **27** was synthesized from 3-hydroxybicyclo[2.2.1]hept-5-ene derivative **29**. We planned to synthesize this intermediate via an enantioselective Diels-Alder reaction. The fluorinated isosteric amines were synthesized from azido diol **30** utilizing Sharpless asymmetric epoxidation^{98,99} of the corresponding fluorinated allylic alcohol, followed by regioselective epoxide opening as described by us previously.¹⁰⁰

The synthesis of tricyclic crown-THF ligand alcohol **27** in optically active form is shown in Scheme 2. As described previously, we utilized a chiral oxazaborolidinium cation



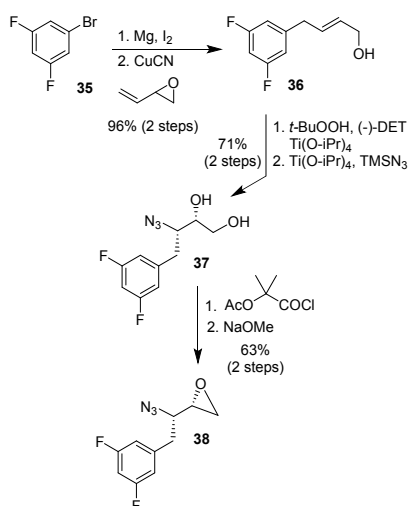
Scheme 1. Synthetic strategies for the preparation of inhibitor **2**

catalyzed Diels-Alder reaction developed by Corey and Mukherjee.^{101,102} The Diels-Alder reaction of readily available ethyl vinyl boronate **31**¹⁰³ and cyclopentadiene afforded the corresponding cycloadduct, which was oxidized with H₂O₂ to furnish optically active alcohol **29** in excellent yield and in excellent optical purity (98% *ee*). Alcohol **29** was then converted to bicyclic acetal **33** in a four-steps to provide bicyclic acetal **33** (2:1 mixture). The lactol mixture was exposed to TFA to provide tricyclic *exo*-alcohol **34** in good yield. This *exo*-alcohol was then converted to *endo*-alcohol **27** by oxidation followed by reduction of the resulting ketone.¹⁰⁴ Crown-THF ligand alcohol, (3*S*,3*aS*,5*R*,7*aS*,8*S*)-hexahydro-4*H*-3,5-methanofuro[2,3-*b*]-pyran-8-ol (**27**) was obtained in good yield. This overall route is efficient and provided access to both *endo*- and *exo*-ligand alcohols in optically active form (>99% *ee*).

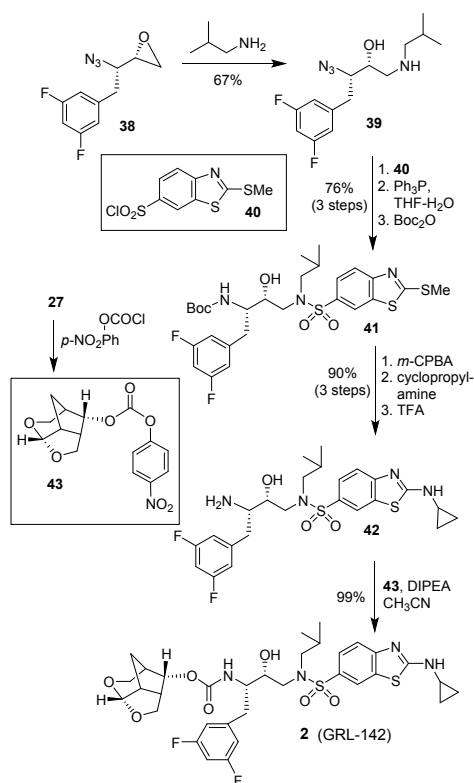


Scheme 2. Synthesis of *Crn*-THF ligand **27**.

Our synthesis of the 3,5-difluorobenzene epoxide derivative for the synthesis of inhibitor **2** is shown in Scheme 2. Commercially available 1-bromo-3,5-difluorobenzene **35** was converted to its 3,5-difluorophenyl magnesium bromide and this Grignard reagent was reacted with butadiene monoxide to provide allylic alcohol **16**.⁶¹ Sharpless asymmetric epoxidation of **16** with (-)-diethyl-D-tartrate resulted in the corresponding epoxide which was reacted with TMSN₃ and Ti(O*i*Pr)₄ to afford the azido diol **37**.^{98,99,105} Diol **37** was then converted to epoxide **38** as described previously.^{106,107}

Scheme 3. Synthesis of difluoroazidoepoxide **38**.

Epoxide **38** was then converted to inhibitor **2** as shown in Scheme 4. Reaction of **38** with isobutylamine provided azidoalcohol **39**. This was then reacted with sulfonyl chloride **40** to provide the sulfonamide, which was converted to Boc amine

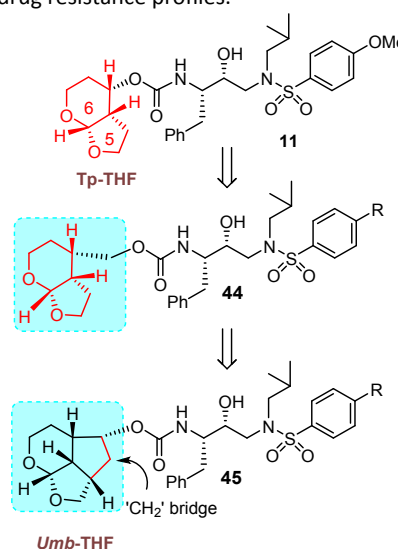
Scheme 4. Synthesis of protease inhibitor **2**.

derivative **41**. Oxidation of the sulfide provided the sulfone, which was then reacted with cyclopropylamine followed by deprotection of Boc with TFA to furnish aminoalcohol **42**. Crown-THF ligand alcohol **27** was converted to activated

carbonate **43** which reacted with amine **42** to furnish inhibitor **2** in good overall yield.^{90,91}

Synthesis of Fused Tricyclic Polyether-derived HIV-1 Protease Inhibitors

Recently, we have designed, synthesized and evaluated another new class of HIV-1 protease inhibitors containing stereochemically defined fused tricyclic polyethers as the P2 ligands and a variety of sulfonamide derivatives as the P2' ligands.¹⁰⁸ As described previously, based upon the X-ray crystal structure of DRV (**1**)-bound HIV-1 protease and its methoxy derivative **10**-bound HIV-1 protease, we have designed hexahydrofurofuran-derived urethane as the P2-ligand in inhibitor **11**, which exhibited enhanced activity over inhibitor **10**.⁷⁴ Inhibitor **11** maintained potent antiviral activity against drug-resistant HIV-1 strains similar to darunavir and its methoxy derivative **10**. In an effort to promote further backbone interactions in the S2 subsite with the bicyclic acetal functionality, we speculated that a methylene group would be more effective. As shown in Figure 17, a hydroxymethyl urethane in inhibitor structure **44** would be optimum for effective contact with the backbone amide NHs. However, we planned to incorporate a methylene bridge to promote stability as shown in inhibitor structure **45**. An inhibitor model shows an increase of the dihedral angle of the acetal template and better alignment with Asp29 and Asp30 backbone amide NHs. The resulting preorganized and conformationally constrained octahydro-2*H*-1,7-dioxacyclopenta[*cd*]indene incorporates three extra methylene groups over *bis*-THF ligand in DRV. This ligand is expected to make more favorable van der Waals interactions since these methylene groups are located in the hydrophobic space surrounding Ile47, Val32, Leu76, and Ile50' residues in the S2 subsite. We presumed that the umbrella-like tetrahydropyranofuran (*Umb*-THF) may show better adaptability to protease mutation. We planned to optimize ligand-binding site interactions of inhibitors with an *Umb*-THF P2 ligand in combination with a fluorinated phenylmethyl P1 ligand and benzothiazole derivatives to improve activity and drug resistance profiles.

Figure 17. Design of *Umb*-THF P2 ligand

We have synthesized a series of inhibitors incorporating *Umb*-THF as the P2 ligand in combination with other P1 and P2' ligands.¹⁰⁸

All inhibitors containing the *Umb*-THF as the P2 ligand provided very potent activity. As can be seen in Figure 18, inhibitor **46** with an (2a*S*,2a1*S*,4*R*,4a*S*,7a*S*)-octahydro-2*H*-1,7-dioxacyclopentaindenyl urethane as the P2 ligand with a 4-methoxybenzenesulfonamide as the P2'-ligand, displayed an enzyme inhibitory K_i of 8 μ M and antiviral IC_{50} value of 9 nM. Interestingly inhibitor **47** with an enantiomeric ligand also showed very potent activity however, both inhibitors displayed reduced antiviral activity compared to inhibitor **10** or **11**. We have also investigated the effect of alternative fused tetrahydrofuranopyran rings in inhibitor **48**. This inhibitor showed a reduction in enzyme and antiviral activity compared to inhibitor **46**.¹⁰⁸

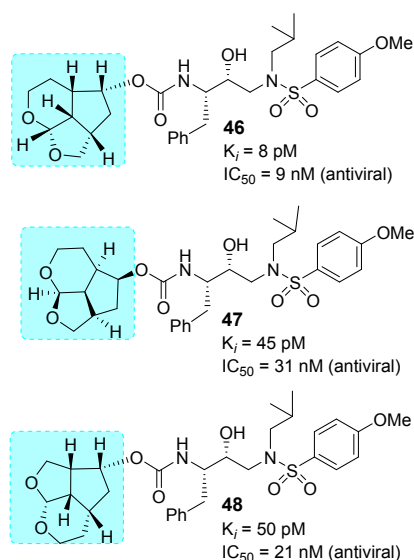


Figure 18. Structure and activity of inhibitors 46-48.

We then examined aminocyclopropylbenzothiazole (Abt) sulfonamide as the P2' ligand. As shown in Figure 19, both inhibitors **49** and **50** with the enantiomeric *Umb*-ligand as the P2 ligand and Abt as the P2' ligand displayed significant improvement in antiviral activity compared to inhibitors **46** and **47** with 4-methoxybenzenesulfonamide as the P2'-ligand. Then, incorporation of a 3,5-difluorobenzyl moiety as the P1 ligand in inhibitors **49** and **50** provided inhibitors **51** and **52** with enantiomeric P2 ligands. Both inhibitors exhibited exceptionally potent activity, displaying antiviral IC_{50} values of 23 μ M for inhibitor **51** and 27 μ M for inhibitor **52**, comparable to Crown-THF-derived inhibitor **2**.

Table 6. Comparison of the antiviral activity of **51** and **52** and other PIs against highly PI-resistant HIV-1 variants.

Virus ^a	EC_{50} (nM) ^a					
	LPV	APV	ATV	DRV	51	52
HIV-1 _{NL4-3}	0.032	0.087	0.0033	0.003	0.002	0.0012
HIV-1 _{ATV^R5μM}}	>1 (>31)	>1 (>11)	>1 (>303)	0.024 (8)	0.0015 (1)	0.0006 (0.3)
HIV-1 _{LPV^R5μM}}	>1 (>31)	0.19 (2)	0.029 (9)	0.026 (9)	0.002 (2)	0.002 (1)
HIV-1 _{APV^R5μM}}	0.39 (12)	>1 (>11)	0.07 (21)	0.2 (67)	0.00032 (0.3)	0.0003 (0.2)

^aThe EC_{50} (50% effective concentration) values were determined by using MT-4 cells as target cells. MT-4 cells (10^5 /mL) were exposed to 100 TCID₅₀s of each HIV-1, and the inhibition of p24 Gag protein production by each drug was used as an endpoint. All assays were conducted in duplicate, and the data shown represent mean values (\pm S.D.) derived from the results of two independent experiments.

We evaluated the antiviral activity of both potent *Umb*-THF-derived inhibitors **51** and **52** against a panel of HIV-1 variants that had been selected *in vitro* with three widely used FDA-approved PI drugs as described previously.^{109,110} The results are shown in Table 6. As can be seen, both inhibitors **51** and **52** maintained exceptional activity against all three HIV-1 variants with EC_{50} values ranging from 0.0003 to 0.002 nM. Essentially, both inhibitors did not show any loss in antiviral activity compared to wild-type HIV_{NL4-3}.

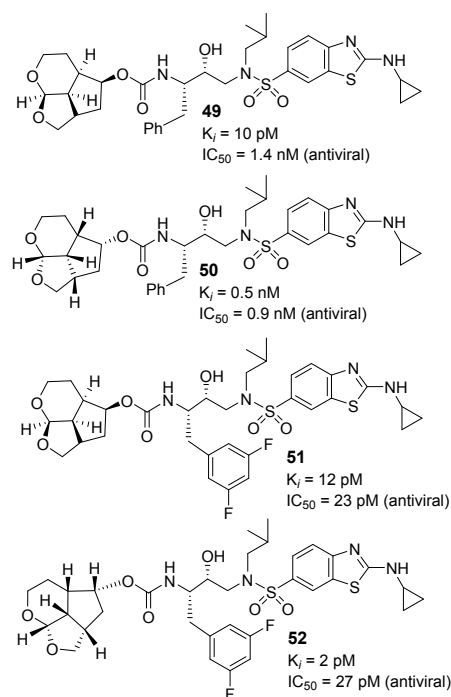


Figure 19. Structure and activity of inhibitors 49-52.

We determined high resolution X-ray crystal structures of both inhibitors **51**- and **52**-bound HIV-1 protease. All key inhibitor-protease interactions are shown in Figure 20. The *Umb*-THF P2 ligand forms stronger hydrogen bonds with backbone atoms in the S2-site. Also, both enantiomeric ligands make enhanced van der Waals interactions in S2-site compared to the *bis*-THF ligand of DRV. The acetal oxygens are suitably positioned and formed strong hydrogen bonds with backbone NHs of Asp29 and Asp30. The *Umb*-THF ligands form significant van der Waals interactions with the side chain atoms of Ile50, Ile47, Val32, and Ile84 in the S2 subsite. The bulging P2 ligand

in **52** is nicely accommodated by shifting the Gly48 carbonyl group in flap region into an alternate conformation. Interestingly, the enantiomeric *Umb*-THF ligand in inhibitor **51** rotated towards the CD1 atom of Ile50 to form a van der Waals contact. These interactions are extensive and they contributed towards the exceptional potency and superior drug resistance properties of inhibitors **51** and **52**.¹⁰⁸

Our synthesis of optically active *Umb*-THF ligand alcohol is shown in Scheme 5. Dihydropyran was converted to bromo ether **13** using NBS and propargyl alcohol. Dehydrobromination of bromo ether provided ene-yne derivative **14**.¹¹¹ Pauson-Khand cyclization^{112,113} of

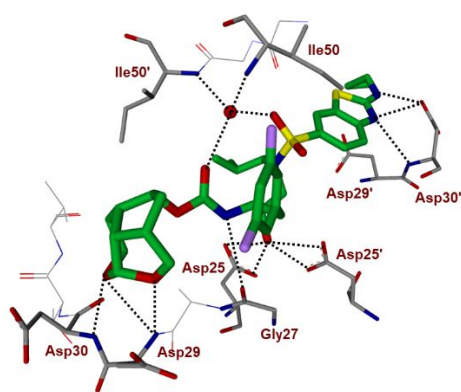


Figure 20A. Inhibitor **52**-bound HIV-1 protease X-ray structure is shown (PDB code: 6CDJ). The inhibitor carbon atoms are shown in green and hydrogen bonds are shown by black dotted lines.

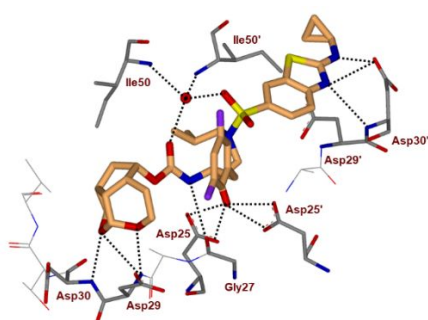
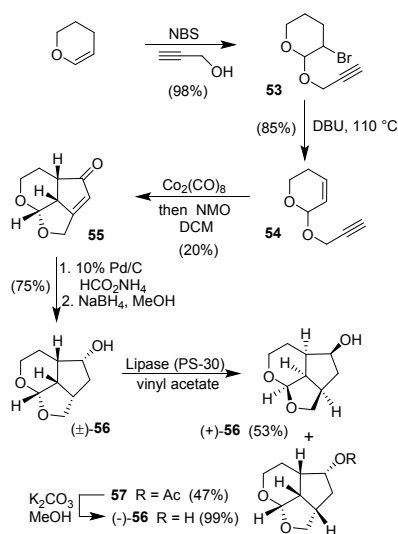


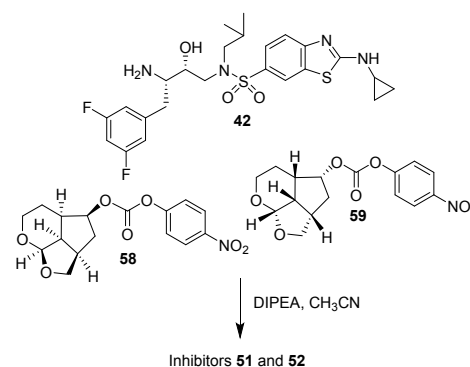
Figure 20B. Inhibitor **51**-bound HIV-1 protease X-ray structure is shown (PDB code: 6CDL). The inhibitor carbon atoms are shown in cyan and hydrogen bonds are shown by black dotted lines.

14 with $\text{CO}_2(\text{CO})_8$ in hexane furnished tricyclic enone **15**. Transfer hydrogenation followed by reduction of the resulting ketone furnished racemic ligand alcohol **16**. Lipase catalyzed enzymatic resolution^{114,115} of racemic alcohol **16** afforded optically active alcohol (+)-**16** and its acetic derivative **17**. Saponification of **17** provided optically active ligand alcohol (-)-**16**.



Scheme 5. Synthesis of optically active ligand alcohol **16**.

Above optically active ligand alcohols were converted to their respective mixed activated carbonate derivatives **18** and **19**. Reaction of these carbonates with amine **42** containing fluorines in the P1 ligand, furnished inhibitors **51** and **52**, respectively. The overall route involving Pauson-Khand cyclization as a key step provided convenient access to various *Umb*-THF ligands for SAR and optimization work.¹⁰⁸ Our preliminary results show that the combination of the fused tricyclic *Umb*-THF as the P2 ligands, a cyclopropylaminobenzothiazole derivative as the P2'-ligand, and a 3,5-difluorophenylmethyl as the P1 ligand resulted in exceptionally potent inhibitors with marked drug resistance profiles. Further optimization of the ligand-binding site interactions based upon the X-ray structures of inhibitor-HIV-1 protease complexes may lead to inhibitors with improved properties.



Scheme 6. Synthesis of inhibitors **51** and **52**.

Recent development of related HIV-1 protease inhibitors from other laboratories.

The design, synthesis, and optimization of protease inhibitors for clinical development continues to be a very active area of research. Darunavir, the last approved protease inhibitor drug, sets a high standard for next generation protease inhibitors. Several laboratories recently reported further structural modification of darunavir scaffold to improve potency and drug-resistance properties. We will report here new and relevant inhibitors since 2016 that are not reported in previous reviews.^{19,57}

Based upon X-ray structures of darunavir-bound HIV-1 protease (PDB ID: 4HLA), we have shown that incorporation of carboxylic acid, carboxamide or stereochemically defined hydroxyl alkyl groups on the P2'-ligand of darunavir led to enhanced hydrogen bonding interactions in the S2'-subsite.¹¹⁶ As shown in Figure 21, compounds **60-62** exhibited very potent protease inhibitory activity, however, they displayed significantly reduced antiviral activity possibly due to efflux properties of these derivatives.^{117,118} X-ray structural studies of **60**-bound HIV-1 protease documented extensive hydrogen bonding interactions in the S2'-site.¹¹⁷ Raines and co-workers reported the design of boronic acid based derivatives and showed extraordinary enhancement of HIV-1 protease inhibitory activity.¹¹⁹ Representative derivatives **63** and **64** showed femtomolar K_i values, however antiviral activity was reduced significantly. X-ray structural studies showed similar enhanced hydrogen bonding interactions as the carboxylic acid derivative **60**. Interestingly, inhibitor **65**, containing *crow*n-THF ligands as the P2 ligand and boronic acid as the P2' ligand showed improved antiviral activity.¹¹⁸ We have examined antiviral

activity of inhibitors **64** and **65** against DRV-resistant HIV-1 variants and the results were compared against darunavir and our recent

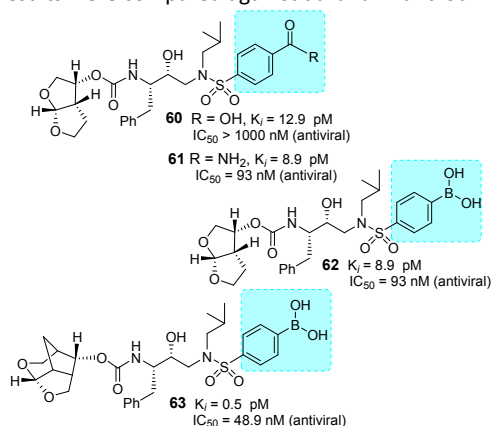


Figure 21. Structure and activity of inhibitors 60–53.

highly potent inhibitor **2** as shown in Table 7.¹¹⁸ All boronic acid and carboxylic acid-derived inhibitors exhibited significantly reduced antiviral activity against the highly DRV-resistant HIV-1 variants.

Table 7. Antiviral activity of inhibitors against highly DRV-resistant HIV-1 variants.

	Mean IC_{50} in nM \pm SD (fold-change)				
	LPV	1	62	63	2 (GRL-142)
HIV _{NL4-3} ^{WT}	13 \pm 2	3.2	48.9	37.7	0.017
HIV _{DRV} ^R _{P20}	>1000 (>77)	525.8 (164)	219.3 (4)	71.2 (2)	0.0024
HIV _{DRV} ^R _{P30}	>1000 (>77)	601 (>187)	946.4 (19)	532.3 (14)	0.14
HIV _{DRV} ^R _{P51}	>1000 (>77)	5429.7 (>1000)	>1000	>1000	1.3

Numbers in parentheses represent fold changes in IC_{50} s for each isolate compared to the IC_{50} s for wild-type cHIV_{NL4-3}^{WT}. All assays were conducted in triplicate.

Besides carboxylic acid and boronic acid functionalities, we and others have explored stereochemically defined hydroxyl groups to make enhanced hydrogen bonding interactions in the S2' site. The effect of these functionalities on the antiviral activity was evaluated. As shown in Figure 22, darunavir derivative **64** with a (*R*)-hydroxyl group on the P2' ligand showed comparable in vitro activity as darunavir. Interestingly, the derivative **65** with (*S*)-isomer showed much reduction in potency.^{27,116} Rusere and co-workers have also investigated the effect of various polar groups on the P2' ligand in combination with other P1' ligands.¹²⁰ As shown in Figure 23, inhibitors **66–69** have shown very potent protease inhibitory activity against drug-resistant variants 184V and I50V/A71V. The X-ray structure of inhibitor **67**-bound HIV-1 protease showed extensive interactions in the S2'-subsite as shown in Figure 24.¹²⁰

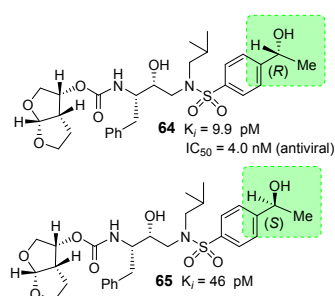


Figure 22. Structure and activity of inhibitors **64** and **65**.

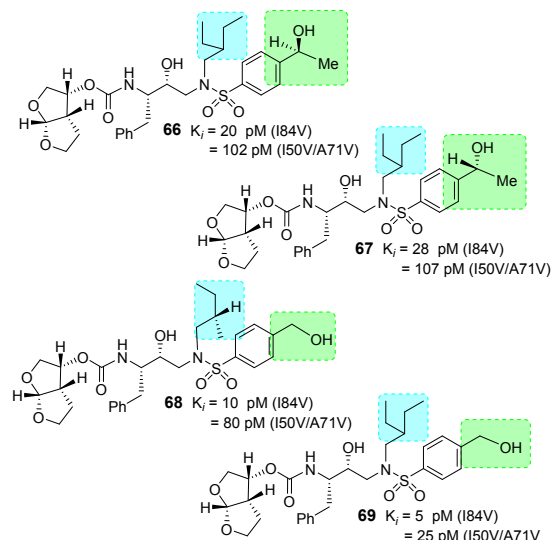


Figure 23. Structure and activity of inhibitors **66–69**.

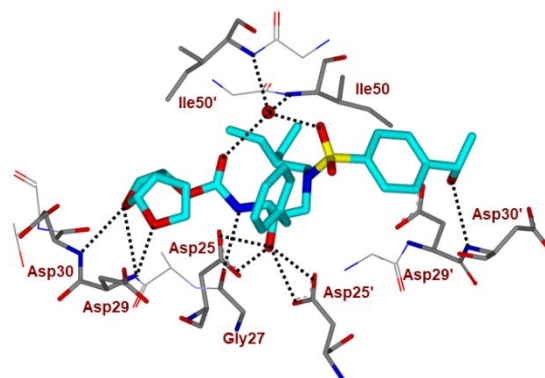


Figure 24. Inhibitor **67**-bound HIV-1 protease X-ray structure is shown (PDB code: 6OXV). The inhibitor carbon atoms are shown in cyan and hydrogen bonds are shown by black dotted lines.

Rusere and co-workers have investigated protease inhibitors incorporating *bis*-tetrahydrofuran as the P2 or P2' ligand in pseudosymmetric dipeptide isosteres related to lopinavir.^{121,122} The authors' structure-activity relationship studies revealed that *bis*-THF carbamate can be incorporated in both sides of the isostere without affecting much of enzyme inhibitory activity. Representative inhibitors **70–73** in Figure 25 showed very potent K_i values against wild-type as well as protease mutants I84V and I50V/A71V. However, antiviral activity of these derivatives is not improved over darunavir or lopinavir. X-ray structural studies have indicated strong hydrogen bonding interactions of the *bis*-THF ligand with backbone amide NHs Asp29 and Asp30 as well as Asp29' and Asp30' NH similar to interactions of *bis*-THF ligand in the S2 subsite of darunavir.¹²¹

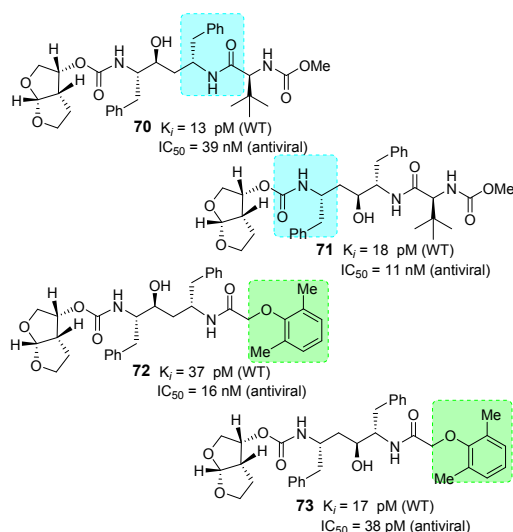


Figure 25. Structure and activity of inhibitors **70-73**.

Bai and co-workers have reported design, synthesis, and structure-activity relationship studies of HIV-1 protease inhibitors incorporating stereochemically defined aminotetrahydrofuran-derived tertiary amine-amide as the P2' ligand in hydroxysulfonamide isostere scaffold.^{123,124} Many amide derivatives were explored and a number of tertiary amide derived inhibitors have shown low nanomolar to subnanomolar HIV-1 protease inhibitory activity. Among representative examples **74-77** in Figure 26, inhibitor **77** with *N*(*S*-tetrahydrofuran)-*N*(2-methoxyethyl)acetamide P2 ligand in combination with 3,4-methylenedioxybenzene sulfonamide P2' ligand exhibited best protease inhibitory activity (IC_{50} 0.35 nM). These derivatives showed low cytotoxicity. However, antiviral activity of these compounds was not reported.¹²³

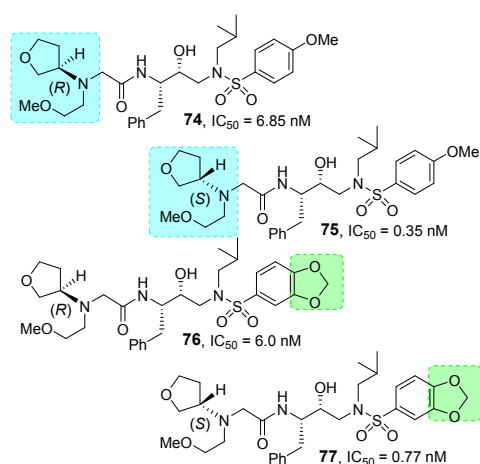


Figure 26. Structure and activity of inhibitors **74-77**.

Bungard and co-workers reported the design and synthesis of a potent series of HIV-1 protease inhibitors containing a piperazine sulfonamide core.^{125,126} The design of these inhibitors was based upon the work of pyrrolidine based inhibitor **78** (Figure 27), reported by Coburn and co-workers.¹²⁷ Presumably, the pyrrolidine NH binds to catalytic Asp25 and Asp25' in the active site. A truncated derivative **79** containing a morpholine was then designed. This compound weakly inhibited HIV-1 protease (11% inhibition at 1 μ M), however,

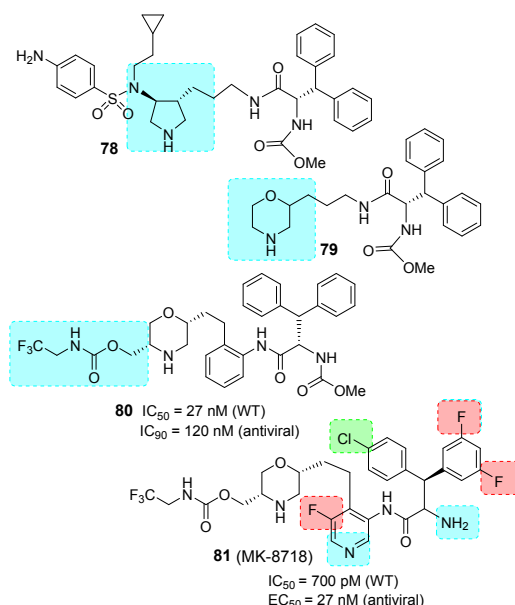


Figure 27. Structure and activity of inhibitors **78-81**.

structural studies of inhibitor-bound HIV-1 protease showed key interactions with catalytic Asp25 and Asp25' in the active site. Also, the two phenyl groups occupied the S1 and S3 regions in the protease active site.

Subsequently, the X-ray structure-based optimization of substituents and incorporation of functionalities were carried out. In inhibitor **80**, an aniline moiety was incorporated on the side chain and a methyl carbamate functionality was introduced on the morpholine ring. Compound **80** displayed low nanomolar HIV-1 protease inhibitory activity and exhibited antiviral IC_{95} value of 120 nM. Rat pharmacokinetic studies showed oral favorable bioavailability for compound **80** (5 mpk, $F = 19\%$). Further optimization of P1, P1', P2 and P3 ligands resulted in Inhibitor **81** (MK 8718) with improved antiviral and pharmacokinetic properties.¹²⁵

Further design based upon the structural information of inhibitor **81**-bound HIV-1 protease led to the development of very potent inhibitors containing piperazine sulfonamide core. As shown in Figure 28, inhibitor **82** exhibited very potent enzyme inhibitory activity (IC_{50} 12 pM) and antiviral activity (EC_{50} 2.8 nM), comparable to darunavir and atazanavir. The X-ray structure of a related inhibitor **83**-bound HIV-1 protease was determined.¹²⁵ As shown in Figure 29, the structure revealed unique modes of interaction with catalytic aspartates as well as interactions of inhibitor's sulfonamide group with Ile50 and Ile50' located in the flaps of HIV-1 protease. The piperazine NH is involved in hydrogen bonding interactions with catalytic Asp25 and Asp25' in the active site.

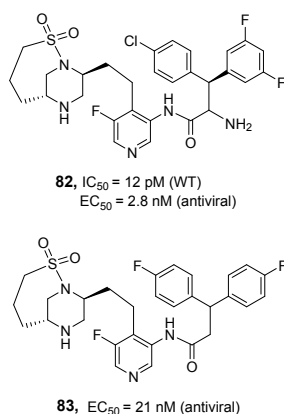


Figure 28. Structure and activity of inhibitors **82** and **83**.

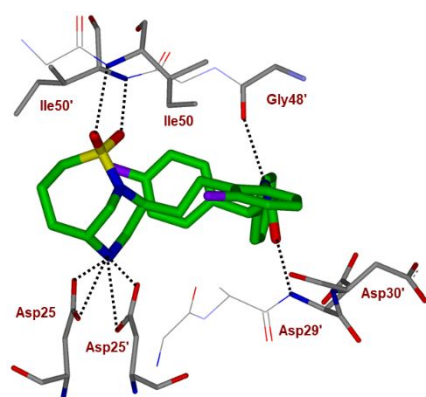


Figure 29. Inhibitor **83**-bound HIV-1 protease X-ray structure is shown (PDB code: 6B3H). The inhibitor carbon atoms are shown in green and hydrogen bonds are shown by black dotted lines.

Conclusion

HIV-1 protease inhibitors continue to play an important role in the current treatment and management of patients with HIV-1 infection and AIDS. The last approved HIV-1 protease inhibitor drug is darunavir, which has become widely used first-line therapy for treatment of HIV/AIDS patients. Darunavir based therapy is particularly effective for treatment of patients harboring multidrug-resistant HIV-1 variants that do not respond to existing ART regimens. Darunavir is conceptually different from other approved protease inhibitor drugs. Darunavir exhibits unprecedented dual mechanism of action, (1) it inhibits catalytically active dimeric HIV-1 protease; (2) it prevents dimerization of protease monomers into the active enzyme. During darunavir design, we incorporated a stereochemically defined *bis*-tetrahydrofuran heterocycle as the P2 ligand in combination with a *p*-aminobenzenesulfonamide as the P2' ligand. These structural features are specifically designed to make extensive hydrogen bonding interactions from S2 and S2' subsites of HIV-1 protease. The 'backbone binding' interactions of darunavir on both sides

of the dimeric protease as well as the polyether structural features of the *bis*-THF ligand are critical to its extraordinary antiviral activity against multidrug-resistant HIV-1 strains.

Since our discovery of darunavir, we have set our focus on the design and development of a new generation of protease inhibitors which can show robust drug-resistant profiles and maintain potency against darunavir and other PI-resistant viruses. Also, we planned to design inhibitors that can cross the blood-brain barrier to inhibit HIV-1 replication in the CNS and reduce developing HAND. In this review, we provided highlights of our recent development of exceptionally potent new generation HIV-1 protease inhibitors that incorporated a host of new polyether-like conformationally constrained polycyclic ligands such as, crown-THF, *Umb*-THF as P2 ligands; aminobenzothiazole and aminobenzoxazole-derived P2' ligands, and fluorinated phenylmethyl derivatives as the P1 ligand to make enhanced backbone binding as well as van der Waals interactions in the active site. Among these inhibitors, inhibitor GRL-142 and related derivatives are particularly very intriguing as these compounds display significantly better antiviral activity, drug-resistance profiles, and drug-like properties compared to darunavir. We feature design principles for cyclic polyether-derived nonpeptide ligands motivated by bioactive natural products, backbone binding design strategies to combat drug resistance, in-depth biological studies including in vitro antiviral studies against a range of MDR variants, and X-ray structural studies of inhibitor-protease complex to gain structural insights into activity and properties. We hope this review will further stimulate design and discovery efforts toward improved treatment against HIV infection and AIDS.

Conflicts of interest

There are no conflicts to declare.

Acknowledgements

This research was supported by the National Institutes of Health (Grant AI150466, AKG and Grant AI150461, ITW). X-ray data were collected at the Southeast Regional Collaborative Access Team (SER-CAT) beamline 22BM at the Advanced Photon Source, Argonne National Laboratory. Use of the Advanced Photon Source was supported by the US Department of Energy, Basic Energy Sciences, Office of Science, under Contract No. W-31-109-Eng-38. This work was also supported by the Intramural Research Program of the Center for Cancer Research, National Cancer Institute, National Institutes of Health (HM), and in part by grants for the promotion of AIDS research from the Ministry of Health, Welfare and Labor of Japan (HM); grants for the Research Program on HIV/AIDS from the Japan Agency for Medical Research and Development (AMED) under grant numbers JP15fk0410001 and JP18fk0410001 (HM); a grant from the National Center for Global Health and Medicine (NCGM) (HM); and grants from JSPS KAKENHI (HM). The authors would like to thank the Purdue University Center for Cancer Research, which supports the shared NMR and mass spectrometry facilities.

Notes and references

- S. G. Deeks, N. Archin, P. Cannon, S. Collins, R. B. Jones, M. A. W. P. de Jong, O. Lambotte, R. Lamplough, T. Ndung'u, J. Sugarman, C. T. Tiemessen, L. Vandekerckhove and S. R. Lewin, The International AIDS Society (IAS) Global Scientific Strategy working group, *Nature Med.* 2021, **27**, 2085-2098.
- T. R. Frieden, K. E. Foti and J. Mermin, *N. Engl. J. Med.* 2015, **373**, 2281-2287.
- UNAIDS/WHO. Global HIV/AIDS Response - Progress Report 2021, November 2021. Available at <http://www.unaids.org/en/resources/publications/2011/>, Last accessed May 2012.
- E. de Clercq, *Int. J. Antimicrob. Agents* 2009, **33**, 307-320.
- F. J. Palella, K. M. Delaney, A. C. Moorman, M. O. Loveless, J. Fuhrer, G. A. Satten, D. J. Aschman and S. D. Holmberg, *New Engl. J. Med.* 1998, **338**, 853-860.
- K. A. Sepkowitz, *N. Engl. J. Med.* 2001, **344**, 1764-1772.
- J. Maenza and C. Flexner, *Am. Fam. Physician* 1998, **57**, 2789-2798.
- S. Moreno, C. F. Perno, P. W. Mallon, G. Behrens, P. Corbeau, J.-P. Routy and G. Darcis, *HIV Medicine* 2019, **20**, 2-12.
- S. G. Deeks, S. R. Lewin and D. V. Havlir, *Lancet* 2013, **382**, 1525-1533.
- C. Logie and T. M. Gadalla, *AIDS Care* 2009, **21**, 742-753.
- L. Waters and M. Nelson, *Int. J. Clin. Pract.* 2007, **61**, 983-990.
- L. Menendez-Arias, *Antiviral Res.* 2010, **85**, 210-231.
- HIV-associated neurocognitive disorder, by R. C. Smail and B. J. Brew, Chapter 7, pages 75-97. In *Handbook of Clinical Neurology*, Vol. 152 (3rd series), The Neurology of HIV Infection, B. J. Brew, Ed; 2018 Elsevier
- J. S. Currier, *Top. Antivir. Med.* 2018, **25**, 133-137.
- M. Vitoria, A. Rangaraj, N. Ford and M. Doherty, *Curr. Opin. HIV and AIDS* 2019, **14**, 143-149.
- A. K. Ghosh, *J. Med. Chem.* 2009, **52**, 2163-2176.
- A. K. Ghosh, *J. Org. Chem.* 2010, **75**, 7967-7989.
- A. K. Ghosh and B. D. Chapsal, Design of the anti-HIV protease inhibitor darunavir. In *Introduction to Biological and Small Molecule Drug Research and Development*; C. R. Ganellin, R. Jefferis, S. Roberts, Eds.; Elsevier: Amsterdam, 2013; pp 355-385.
- A. K. Ghosh, H. L. Osswald and G. Prato, *J. Med. Chem.* 2016, **59**, 5172-5208.
- A. K. Ghosh, Z. L. Dawson and H. Mitsuya, *Bioorg. Med. Chem.* 2007, **15**, 7576-7580.
- Y. Koh, H. Nakata, K. Maeda, H. Ogata, G. Bilcer, T. Devasamudram, J. F. Kincaid, P. Boross, Y.-F. Wang, Y. Tie, P. Volarath, L. Gaddis, R. W. Harrison, I. T. Weber, A. K. Ghosh and H. Mitsuya, *Antimicrob. Agents Chemother.* 2003, **47**, 3123-3129.
- S. de Meyer, H. Azijn, D. Surleraux, D. Jochmans, A. Tahri, R. Pauwels, P. Wigerinck and M.-P. de Bethune, *Antimicrob. Agents Chemother.* 2005, **49**, 2314-2321.
- E. D. Deeks, *Drugs* 2014, **74**, 99-125.
- On June 23, 2006, FDA approves darunavir for previously treated HIV-infected patients, and in December 13, 2008, for all HIV/AIDS patients including pediatrics who did not receive antiretroviral therapies previously. Available at: http://www.accessdata.fda.gov/drugsatfda_docs/label/2008/021976s009lbl.pdf (accessed May 2012).
- A. Curran and E. R. Pascuet, *Enferm. Infecc. Microbiol. Clin.* 2008, **10**, 14-22.
- A. M. Mills, M. Nelson, D. Jayaweera, K. Ruxrungtham, I. Cassetti, P.-M. Girard, C. Workman, I. Dierynck, V. Sekar, C. V. Abeele and L. Lavreys, *AIDS* 2009, **23**, 1679-1688.
- A. K. Ghosh, P. R. Sridhar, N. Kumaragurubaran, Y. Koh, I. T. Weber and H. Mitsuya, *ChemMedChem* 2006, **1**, 939-950.
- A. K. Ghosh, B. D. Chapsal and H. Mitsuya, Darunavir, a New PI with Dual Mechanism: from a Novel Drug Design Concept to New Hope against Drug-Resistant HIV. In *Aspartic Acid Proteases as Therapeutic Targets*; Ghosh, A. K., Ed.; Wiley-VCH Verlag GmbH & Co. KGaA: Weinheim, Germany, 2010; Vol. 45, pp 205-243.
- A. K. Ghosh, B. D. Chapsal, I. T. Weber and H. Mitsuya, *Acc. Chem. Res.* 2008, **41**, 78-86.
- Y. Tie, P. I. Boross, Y. F. Wang, L. Gaddis, A. K. Hussain, S. Leshchenko, A. K. Ghosh, J. M. Louis, R. W. Harrison and I. T. Weber, *J. Mol. Biol.* 2004, **338**, 341-352.
- A. Y. Kovalevsky, F. Liu, S. Leshchenko, A. K. Ghosh, J. M. Louis, R. W. Harrison and I. T. Weber, *J. Mol. Biol.* 2006, **363**, 161-173.
- K. Yoshimura, R. Kato, M. F. Kavlick, A. Nguyen, V. Maroun, K. Maeda, K. A. Hussain, A. K. Ghosh, S. V. Gulnik, J. W. Erickson and H. Mitsuya, *J. Virol.* 2002, **76**, 1349-1358.
- A. K. Ghosh and S. Gemma, Development of Direct Thrombin Inhibitor, Dabigatran Etxilate, as an Anticoagulant Drug. In *Structure-Based Design of Drugs and Other Bioactive Molecules: Tools and Strategies*; Wiley-VCH: Weinheim, Germany, 2014; pp 337-354.
- A. K. Ghosh, D. D. Anderson, I. T. Weber and H. Mitsuya, *Angew. Chem., Int. Ed.* 2012, **51**, 1778-1802.
- L. Hong, X. Zhang, J. A. Hartsuck and J. Tang, *Protein Sci.* 2000, **9**, 1898-1904.
- G. S. Laco, C. Schalk-Hihi, J. Lubkowski, G. Morris, A. Zdanov, A. Olson, J. H. Elder, A. Wlodawer and A. Gustchina, *Biochemistry* 1997, **36**, 10696-10708.
- A. K. Ghosh and B. Chapsal, Second-Generation Approved HIV-1 Protease Inhibitors for the treatment of HIV/AIDS. In *Aspartic Acid Proteases as Therapeutic Targets*; Ghosh, A. K., Ed.; Wiley-VCH Verlag GmbH & Co. KGaA: Weinheim, Germany, 2010; Vol. 45, pp 169-204.
- D. J. Newman and G. M. Cragg, *J. Nat. Prod.* 2012, **75**, 311-335.
- J. W.-H. Li and J. C. Vederas, *Science* 2009, **325**, 161-165.
- J. Clardy and C. Walsh, *Nature* 2004, **432**, 829-837.
- K. Nakanishi, *Bioorg. Med. Chem.* 2005, **13**, 4987-5000.
- E. Quinoa, Y. Kakou and P. Crews, *J. Org. Chem.* 1988, **53**, 3642-3644.
- D. G. Corley, R. Herb, R. E. Moore, P. J. Scheuer and V. J. Paul, *J. Org. Chem.* 1988, **53**, 3644-3646.
- P. R. Zanno, I. Miura, K. Nakanishi and D. L. Elder, *J. Am. Chem. Soc.* 1975, **97**, 1975-1977.
- J. Wang, S. M. Soisson, K. Young, W. Shoop, S. Kodali, A. Galgocsi, R. Painter, G. Parthasarathy, Y. S. Tang, R. Cummings, S. Ha, K. Dorso, M. Motyl, H. Jayasuriya, J. Ondeyka, K. Herath, C. Zhang, L. Hernandez, J. Allocco, A. Basilio, J. R. Tormo, O. Genilloud, F. Vicente, F. Pelaez, L. Colwell, S. H. Lee, B. Michael, T. Felcetto, C. Gill, L. L. Silver, J. D. Hermes, K. Bartizal, J. Barrett, D. Schmatz, J. W. Becker, D. Cully and S. B. Singh, *Nature* 2006, **441**, 358-361.
- S. B. Singh and J. F. Barrett, *Biochem. Pharmacol.* 2006, **71**, 1006-1015.
- M. J. Towle, K. A. Salvato, J. Budrow, B. F. Wels, G. Kuznetsov, K. K. Aalfs, S. Welsh, W. Zheng, B. M. Seletsky, M. H. Palme, G. J. Habgood, L. A. Singer, L. V. DiPietro, Y. Wang, J. J. Chen, D. A. Quincy, A. Davis, K. Yoshimatsu, Y. Kishi, M. J. Yu and B. A. Littlefield, *Cancer Res.* 2001, **61**, 1013-1021.
- S. B. Singh, J. G. Ondeyka, K. B. Herath, C. Zhang, H. Jayasuriya, D. L. Zink, G. Parthasarathy, J. W. Becker, J. Wang and S. M. Soisson, *Bioorg. Med. Chem. Lett.* 2009, **19**, 4756-4759.
- E. Martens and A. L. Demain, *J. Antibiot.* 2011, **64**, 705-710.
- A. E. Prota, K. Bargsten, P. T. Northcote, M. Marsh, K.-H. Altmann, J. H. Miller, J. F. Diaz and M. O. Steinmetz, *Angew. Chem. Int. Ed. Engl.* 2014, **53**, 1621-1625.

- 51 J. D. Rudolf, L.-B. Dong and B. Shen, *Biochem. Pharmacol.* 2017, **133**, 139-151.
- 52 D. J. Craik, D. P. Fairlie, S. Liras and D. Price, *Chem. Biol. Drug Design* 2012, **81**, 136-147.
- 53 L. Otvos, Jr., J. D. Wade, *Front. Chem.* 2014, **2**, 62.
- 54 W. A. O'Brien III, *AIDS Read.* 2006, **16**, 38-44.
- 55 N. A. Roberts, J. A. Martin, D. Kinchington, A. V. Broadhurst, J. C. Craig, I. B. Duncan, S. A. Galpin, B. K. Handa, J. Kay, A. Kröhn, R. W. Lambert, J. H. Merrett, J. S. Mills, K. E. Parkes, S. Redshaw, A. J. Ritchie, D. L. Taylor, G. J. Thomas and P. J. Machin, *Science* 1990, **248**, 358-361.
- 56 A. K. Ghosh, D. D. Anderson and H. Mitsuya, The FDA approved HIV-1 protease inhibitors for treatment of HIV/AIDS. In *Burger's Medicinal Chemistry, Drug Discovery and Development*, 7th ed.; Abraham, D. J., Rotella, D. P., Eds.; 2010; Vol. 7, pp 1-72.
- 57 Z. Lv, Y. Chu and Y. Wang, *HIV AIDS (Auckl.)* 2015, **7**, 95-104.
- 58 A. K. Ghosh, W. J. Thompson, H. Y. Lee, S. P. McKee, P. M. Munson, T. T. Duong, P. L. Darke, J. A. Zugay, E. A. Emini, W. A. Schleif, J. R. Huff and P. S. Anderson, *J. Med. Chem.* 1993, **36**, 924-927.
- 59 A. K. Ghosh, H. Y. Lee, W. J. Thompson, C. Culberson, M. K. Holloway, S. P. McKee, P. M. Munson, T. T. Duong, A. M. Smith, P. L. Darke, J. A. Zugay, E. A. Emini, W. A. Schleif, J. R. Huff and P. S. Anderson, *J. Med. Chem.* 1994, **37**, 1177-1188.
- 60 A. K. Ghosh, W. J. Thompson, P. M. Munson, W. Liu and J. R. Huff, *Bioorg. Med. Chem. Lett.* 1995, **5**, 83-88.
- 61 A. K. Ghosh, J. F. Kincaid, D. E. Walters, Y. Chen, N. C. Chaudhuri, W. J. Thompson, C. Culberson, P. M. D. Fitzgerald, H. Y. Lee, S. P. McKee, P. M. Munson, T. T. Duong, P. L. Darke, J. A. Zugay, W. A. Schleif, M. G. Axel, J. Lin and J. R. Huff, *J. Med. Chem.* 1996, **39**, 3278-3290.
- 62 A. K. Ghosh, J. F. Kincaid, W. Cho, D. E. Walters, K. Krishnan, K. A. Hussain, Y. Koo, H. Cho, C. Rudall, L. Holland and J. Buthod, *Bioorg. Med. Chem. Lett.* 1998, **8**, 687-690.
- 63 A. K. Ghosh, E. Pretzer, H. Cho, K. A. Hussain and N. Duzgunes, *Antivir. Res.* 2002, **54**, 29-36.
- 64 J. W. Erickson, Anonymous; S. V. Gulnik, H. Mitsuya and A. K. Ghosh, *Fitness Assay and Associated Methods*. US 07470506, 2008.
- 65 S. V. Gulnik, L. I. Suvorov, B. S. Liu, B. Yu, B. Anderson, H. Mitsuya and J. W. Erickson, *Biochemistry* 1995, **34**, 9282-9287.
- 66 K. Yoshimura, R. Kato, M. F. Kavlick, A. Nguyen, V. Maroun, K. Maeda, K. A. Hussain, A. K. Ghosh, S. V. Gulnik, J. W. Erickson and H. A. Mitsuya, *J. Virol.* 2002, **76**, 1349-1358.
- 67 A. K. Ghosh, S. Kulkarni, D. D. Anderson, L. Hong, A. Baldrige, Y.-F. Wang, A. A. Chumanevich, A. Y. Kovalevsky, Y. Tojo, M. Amano, Y. Koh, J. Tang, I. T. Weber and H. Mitsuya, *J. Med. Chem.* 2009, **52**, 7689-7705.
- 68 E. Lefebvre and C. A. Schiffer, *AIDS Rev.* 2008, **10**, 131-142.
- 69 Y. Koh, M. Aoki, M. L. Danish, H. Aoki-Ogata, M. Amano, D. Das, R. W. Shafer, A. K. Ghosh and H. Mitsuya, *J. Virol.* 2011, **85**, 10079-10089.
- 70 H. Hayashi, N. Takamune, T. Nirasawa, M. Aoki, Y. Morishita, D. Das, Y. Koh, A. K. Ghosh, S. Misumi and H. Mitsuya, *Proc. Natl. Acad. Sci. U. S. A.* 2014, **111**, 12234-12239.
- 71 R. S. Yedidi, H. Garimella, M. Aoki, H. Aoki-Ogata, D. V. Desai, S. B. Chang, D. A. Davis, W. S. Fyvie, J. D. Kaufman, D. D. W. Smith, D. Das, P. T. Wingfield, K. Maeda, A. K. Ghosh and H. Mitsuya, *Antimicrob. Agents Chemother.* 2014, **58**, 3679-3688.
- 72 A. Gustchina, C. Sansom, M. Prevost, J. Richelle, S. Y. Wodak, A. Wlodawer and I. T. Weber, *Protein Eng.* 1994, **7**, 309-316.
- 73 A. Wlodawer, M. Miller, M. Jaskólski, B. K. Sathyanarayana, E. Baldwin, I. T. Weber, L. M. Selk, L. Clawson, J. Schneider and S. B. H. Kent, *Science* 1989, **245**, 616-621.
- 74 A. K. Ghosh, B. D. Chapsal, A. Baldrige, M. P. Steffey, D. E. Walters, Y. Koh, M. Amano and H. Mitsuya, *J. Med. Chem.* 2011, **54**, 622-634.
- 75 A. K. Ghosh, S. Yashchuk, A. Mizuno, N. Chakraborty, J. Agniswamy, Y. F. Wang, M. Aoki, P. M. Gomez, M. Amano, I. T. Weber and H. Mitsuya, *ChemMedChem* 2015, **10**, 107-115.
- 76 P. M. Salcedo Gomez, M. Amano, S. Yashchuk, A. Mizuno, D. Das, A. K. Ghosh and H. Mitsuya, *Antimicrob. Agents Chemother.* 2013, **57**, 6110-6121.
- 77 A. K. Ghosh, C. X. Xu, K. V. Rao, A. Baldrige, J. Agniswamy, Y. F. Wang, I. T. Weber, M. Aoki, S. G. Miguel, M. Amano and H. Mitsuya, *ChemMedChem* 2010, **5**, 1850-1854.
- 78 M. Amano, Y. Tojo, P. M. Salcedo-Gomez, J. R. Campbell, D. Das, M. Aoki, C. X. Xu, K. V. Rao, A. K. Ghosh and H. Mitsuya, *Antimicrob. Agents Chemother.* 2013, **57**, 2036-2046.
- 79 A. K. Ghosh, P. R. Sridhar, S. Leshchenko, A. K. Hussain, J. Li, A. Y. Kovalevsky, D. E. Walters, J. E. Wedekind, V. Grum-Tokars, D. Das, Y. Koh, K. Maeda, H. Gatanaga, I. T. Weber and H. Mitsuya, *J. Med. Chem.* 2006, **49**, 5252-5261.
- 80 Y. Koh, D. Das, S. Leschenko, H. Nakata, H. Ogata-Aoki, M. Amano, M. Nakayama, A. K. Ghosh and H. Mitsuya, *Antimicrob. Agents Chemother.* 2009, **53**, 997-1006.
- 81 A. K. Ghosh, S. Gemma, J. Takayama, A. Baldrige, S. Leshchenko-Yashchuk, H. B. Miller, Y. F. Wang, A. Y. Kovalevsky, Y. Koh, I. T. Weber and H. Mitsuya, *Org. Biomol. Chem.* 2008, **6**, 3703-3713.
- 82 N. S. Delino, M. Aoki, H. Hayashi, S.-I. Hattori, S. B. Chang, Y. Takamatsu, C. D. Martyr, D. Das, A. K. Ghosh and H. Mitsuya, *Antimicrob. Agents Chemother.* 2018, **62**, e02060-17.
- 83 A. K. Ghosh, K. V. Rao, P. R. Nyalapatla, H. L. Osswald, C. D. Martyr, M. Aoki, H. Hayashi, J. Agniswamy, Y. F. Wang, H. Bulut, D. Das, I. T. Weber and H. Mitsuya, *J. Med. Chem.* 2017, **60**, 4267-4278.
- 84 M. Amano, P. M. Salcedo-Gomez, R. S. Yedidi, N. S. Delino, H. Nakata, K. V. Rao, A. K. Ghosh and H. Mitsuya, *Sci. Rep.* 2017, **71**, 12235.
- 85 J. Agniswamy, D. W. Kneller, A. K. Ghosh and I. T. Weber, *Biochem. Biophysical. Res. Comm.* 2021, **566**, 30-35.
- 86 R. Ali and N. Siddiqui, *J. Chem.* 2013, **2013**, 345198.
- 87 Seth, S. *Antiinflamm. Antiallergy Agents Med. Chem.* 2015, **14**, 98-112.
- 88 B. K. Park, N. R. Kitteringham and P. M. O'Neill, *Annu. Rev. Pharmacol. Toxicol.* 2001, **41**, 443-470.
- 89 B. E. Smart, *J. Fluor. Chem.* 2001, **109**, 3-11.
- 90 A. K. Ghosh, K. V. Rao, P. R. Nyalapatla, S. Kovala, M. Brindisi, H. L. Osswald, B. Sekhara Reddy, J. Agniswamy, Y. F. Wang, M. Aoki, S. I. Hattori, I. T. Weber and H. Mitsuya, *ChemMedChem* 2018, **13**, 803-815.
- 91 M. Aoki, H. Hayashi, K. V. Rao, D. Das, N. Higashi-Kuwata, H. Bulut, H. Aoki-Ogata, Y. Takamatsu, R. S. Yedidi, D. A. Davis, S. I. Hattori, N. Nishida, K. Hasegawa, N. Takamune, P. R. Nyalapatla, H. L. Osswald, H. Jono, H. Saito, R. Yarchoan, S. Misumi, A. K. Ghosh and H. Mitsuya, *eLife* 2017, **6**, e28020.
- 92 S.-I. Hattori, H. Hayashi, H. Bulut, K. V. Rao, P. R. Nyalapatla, K. Hasegawa, M. Aoki, A. K. Ghosh and H. Mitsuya, *Antimicrob. Agents Chemother.* 2019, **63**, e02635-18.
- 93 H. Bulut, S.-i. Hattori, H. Aoki-Ogata, H. Hayashi, D. Das, M. Aoki, D. A. Davis, K. V. Rao, P. R. Nyalapatla, A. K. Ghosh and H. Mitsuya, *Sci. Rep.* 2020, **10**, 10664.
- 94 Y. Koh, M. Amano, T. Towata, M. Danish, S. Leshchenko-Yashchuk, D. Das, M. Nakayama, Y. Tojo, A. K. Ghosh and H. Mitsuya, *J. Virol.* 2010, **84**, 11961-11969.
- 95 M. Aoki, H. Hayashi, R. S. Yedidi, C. D. Martyr, Y. Takamatsu, H. Aoki-Ogata, T. Nakamura, H. Nakata, D. Das, Y. Yamagata, A. K. Ghosh and H. Mitsuya, *J. Virol.* 2016, **90**, 2180-2194.
- 96 A. K. Ghosh, B. D. Chapsal, A. Baldrige, K. Ide, Y. Koh and H. Mitsuya, *Org. Lett.* 2008, **10**, 5135-5138.

- 97 A. K. Ghosh, B. D. Chapsal, G. L. Parham, M. Steffey, J. Agniswamy, Y.-F. Wang, M. Amano, I. T. Weber and H. Mitsuya, *J. Med. Chem.* 2011, **54**, 5890-5901.
- 98 T. Katsuki and K. B. Sharpless, *J. Am. Chem. Soc.* 1980, **102**, 5974-5976.
- 99 Y. Gao, R. M. Hanson, J. M. Klunder, S. Y. Ko, H. Masamue and K. B. Sharpless, *J. Am. Chem. Soc.* 1987, **109**, 5765-5780.
- 100 A. K. Ghosh, G. E. Schiltz, L. N. Rusere, H. L. Osswald, D. E. Walters, M. Amano and H. Mitsuya, *Org. Biomol. Chem.* 2014, **12**, 6842-6854.
- 101 S. Mukherjee and E. J. Corey, *Org. Lett.* 2010, **12**, 1024-1027.
- 102 K. M. Reddy, E. Bhimireddy, B. Thirupathi, S. Breitler, S. Yu and E. J. Corey, *J. Am. Chem. Soc.* 2016, **138**, 2443-2453.
- 103 J.-E. Lee, J. Kwon and J. Yun, *Chem. Commun.* 2008, **6**, 733-734.
- 104 K. C. Nicolaou, V. A. Adsool and C. R. H. Hale, *Org. Lett.* 2010, **12**, 1552-1555.
- 105 M. Caron, K. Carlier and K. B. Sharpless, *J. Org. Chem.* 1988, **53**, 5185-5187.
- 106 A. K. Ghosh, S. P. McKee, H. Y. Lee and W. T. Thompson, *J. Chem. Soc. Chem. Commun.* 1992, **1992**, 273-274.
- 107 A. K. Ghosh, E. L. Cardenas and M. Brindisi, *Tetrahedron Lett.* 2017, **58**, 4062-4065.
- 108 A. K. Ghosh, P. R. Nyalapatla, S. Kovala, K. V. Rao, M. Brindisi, H. L. Osswald, M. Amano, M. Aoki, J. Agniswamy, Y.-F. Wang, I. T. Weber and H. Mitsuya, *J. Med. Chem.* 2018, **61**, 4561-4577.
- 109 Y. Koh, M. Amano, T. Towata, M. Danish, S. Leshchenko-Yashchuk, D. Das, M. Nakayama, Y. Tojo, A. K. Ghosh and H. Mitsuya, *J. Virol.* 2010, **84**, 11961-11969.
- 110 M. Aoki, M. L. Danish, H. Aoki-Ogata, M. Amano, K. Ide, D. Das, Y. Koh and H. Mitsuya, *J. Virol.* 2012, **86**, 13384-13396.
- 111 J. P. Dulcere, J. Crandal, R. Faure, M. Santelli, V. Agati and M. N. Mihoubi, *J. Org. Chem.* 1993, **58**, 5702-5708.
- 112 S. Shambayati, W. E. Crewel and S. L. Schreiber, *S. L. Tetrahedron Lett.* 1990, **31**, 5289-5292.
- 113 K. M. Brummond and J. L. Kent, *Tetrahedron* 2000, **56**, 3263-3283.
- 114 A. K. Ghosh and Y. Chen, *Tetrahedron Lett.* 1995, **36**, 505-508.
- 115 D. Bianchi, P. Cesti and E. Battistel, *J. Org. Chem.* 1988, **53**, 5531-34.
- 116 A. K. Ghosh, W. S. Fyvie, M. Brindisi, M. Steffey, J. Agniswamy, Y.-F. Wang, M. Aoki, M. Amano, I. T. Weber and H. Mitsuya, *ChemMedChem* **2017**, **12**, 1942-1952.
- 117 R. S. Yedidi, K. Maeda, W. S. Fyvie, M. Steffey, D. A. Davis, I. Palmer, M. Aoki, J. D. Kaufman, S. J. Stahl, H. Garimella, D. Das, P. T. Wingfield, A. K. Ghosh and H. Mitsuya, *Antimicrob. Agents Chemother.* **2013**, **57**, 4920-4927.
- 118 A. K. Ghosh, Z. Xia, S. Kovala, W. L. Robinson, M. E. Johnson, D. W. Kneller, Y.-F. Wang, M. Aoki, Y. Takamatsu, I. T. Weber and H. Mitsuya, *ChemMedChem* **2019**, **14**, 1863-1872.
- 119 I. W. Windsor, M. J. Palte, J. C. Lukesh III, B. Gold, K. T. Forest and R. T. Raines, *J. Am. Chem. Soc.* **2018**, **140**, 14015-14018.
- 120 L. N. Rusere, G. J. Lockbaum, S.-K. Lee, M. Henes, K. Kosovrasti, E. Spielvogel, E. A. Nalivaika, R. Swanstrom, N. K. Yilmaz, C. A. Schiffer and A. Ali, *J. Med. Chem.* **2019**, **62**, 8062-8079.
- 121 L. N. Rusere, G. J. Lockbaum, M. Henes, S.-K. Lee, E. Spielvogel, D. N. Rao, K. Kosovrasti, E. A. Nalivaika, R. Swanstrom, N. K. Yilmaz, C. A. Schiffer and A. Ali, *J. Med. Chem.* **2020**, **63**, 8296-8319.
- 122 X. Chen, L. Li, D. J. Kempf, H. Sham, N. E. Wideburg, A. Saldivar, S. Vasavanonda, K. C. Marsh, E. McDonald and D. W. Norbeck, *Bioorg. Med. Chem. Lett.* **1996**, **6**, 2847-2852.
- 123 X. Bai, Z. Yang, M. Zhu, B. Dong, L. Zhou, G. Zhang, J. Wang and Y. Wang, *Eur. J. Med. Chem.* **2017**, **137**, 30-44.
- 124 Z.-H. Yang, X.-G. Bai, L. Zhou, J.-X. Wang, H.-T. Liu and Y.-C. Wang, *Bioorg. Med. Chem. Lett.* **2015**, **25**, 1880-1883.
- 125 C. J. Bungard, P. D. Williams, J. Schulz, C. M. Wiscourt, M. K. Holloway, H. M. Loughran, J. J. Manikowski, H.-P. Su, D. J. Bennett, L. Chang, X.-J. Chu, A. Crespo, M. P. Dwyer, K. Keertikar, G. J. Morriello, A. W. Stamford, S. T. Waddell, B. Zhong, B. Hu, T. Ji, T. L. Diamond, C. Bahnck-Teets, S. S. Carroll, J. F. Fay, X. Min, W. Morris, J. E. Ballard, M. D. Miller and J. A. McCauley, *ACS Med. Chem. Lett.* **2017**, **8**, 1292-1297.
- 126 C. J. Bungard, P. D. Williams, J. E. Ballard, D. J. Bennett, C. Beaulieu, C. Bahnck-Teets, S. S. Carroll, R. K. Chang, D. C. Dubost, J. F. Fay, T. L. Diamond, T. J. Greshock, L. Hao, M. K. Holloway, P. J. Felock, J. J. Gesell, H.-P. Su, J. J. Manikowski, D. J. McKay, M. Miller, X. Min, C. Molinaro, O. M. Moradei, P. G. Nantermet, C. Nadeau, R. I. Sanchez, T. Satyanarayana, W. D. Shipe, S. K. Singh, V. L. Truong, S. Vijayasradhi, C. M. Wiscourt, J. P. Vacca, S. N. Crane, and J. A. McCauley, *ACS Med. Chem. Lett.* **2016**, **7**, 702-707.
- 127 C. A. Coburn, M. K. Holloway, J. P. Vacca, Preparation of phenylsulfonylpyrrolidinylaminoethyl diphenylalaninamides as HIV protease inhibitors. WO2010138338A1, 2010.



Arun K. Ghosh received his BS and MS in Chemistry from the University of Calcutta and Indian Institute of Technology, Kanpur respectively. He obtained his PhD in 1985 at the University of Pittsburgh. He pursued postdoctoral research with Professor E. J. Corey at Harvard University (1985-1988). He was a research fellow at Merck Research Laboratories prior to joining the University of Illinois-Chicago as an assistant Professor in 1994. In 2005, he moved to Purdue University where he is currently the Ian P. Rothwell Distinguished Professor in Chemistry and Medicinal Chemistry. His research interests are in the areas of organic, bioorganic, drug-design, and medicinal chemistry.



Hiroaki Mitsuya received his MD and PhD from National Kumamoto University School of Medicine (Japan). Following training in oncology/hematology/immunology, he joined National Cancer Institute in Bethesda (USA) in 1982, where he has been Principal Investigator & Chief of Experimental Retrovirology Section since 1991 to present. He also served as Professor of Medicine and Chairman of Departments of Hematology/Rheumatology/Infectious Diseases at Kumamoto University from 1997 to 2016. He now serves as Director, National Center for Global Health & Medicine, Tokyo. His current research focuses on antiviral research for development of therapeutics for HIV/AIDS, hepatitis B, and SARS-CoV-2.



Irene T. Weber received her BS and MS from Cambridge University, England, and obtained her PhD in 1978 from Oxford University, England. She pursued postdoctoral research with Professor Thomas Steitz at Yale University. She was Professor of Microbiology and Immunology at Thomas Jefferson University in Philadelphia from 1991. She moved to Georgia State University, Atlanta, in 2001 where she is a Regents' Professor of Biology and Chemistry and Georgia Cancer Coalition Distinguished Cancer Scientist. Her research focuses on the structure and activity of enzymes.